

Optical effects of proposed iron-sand mining in the South Taranaki Bight region - worst case update

April 2017

Prepared for Trans-Tasman Resources Ltd



Authors/Contributors:

Matt Pinkerton

For any information regarding this report please contact:

Matt Pinkerton

Principal Scientist

m.pinkerton@niwa.co.nz

National Institute of Water & Atmospheric Research Ltd

Private Bag 14901

Kilbirnie



Wellington 6241

Phone +64 4 386 0300

NIWA Client Report No: 2017089WNrev1

Report date: April 2017

NIWA Project: TTR17301

| Quality Assurance Statement | | |
|---|--------------------------|-------------------|
|  | Reviewed by: | Alison MacDiarmid |
|  | Approved for release by: | Alison MacDiarmid |

Cover image: Pseudo-true colour MODIS-Aqua satellite image of the South Taranaki Bight (29 April 2011). Data used courtesy of NASA, Goddard Space Flight Center, MODIS project.

Contents

| | |
|---|-----------|
| Executive summary | 7 |
| 1 Introduction | 8 |
| 1.1 TTR iron-sand mining proposal | 8 |
| 2 Predicted optical effects..... | 9 |
| 2.2 Descriptive transects | 9 |
| 2.3 Euphotic zone depth | 10 |
| 2.4 Horizontal visibility (Black disk distance) | 14 |
| 2.5 Water colour | 18 |
| 2.6 Water column light intensity | 18 |
| 2.7 Light at the seabed | 22 |
| 2.8 Optical effects at selected sites | 27 |
| 2.9 Discussion and conclusions..... | 43 |
| 3 Acknowledgements | 46 |
| 4 References..... | 46 |

Tables

| | | |
|-------------|--|----|
| Table 2-10: | Modelled effect of mining on water column light. | 19 |
| Table 2-11: | Predicted changes to optical properties. | 26 |
| Table 2-1: | Locations and approximate water depths in proposed monitoring locations. | 27 |
| Table 2-2: | Source A to Whanganui 20: Predicted optical properties. | 29 |
| Table 2-3: | Graham Bank: Predicted optical properties. | 31 |
| Table 2-4: | The Crack 1: Predicted optical properties. | 33 |
| Table 2-5: | The Crack 2: Predicted optical properties. | 35 |
| Table 2-6: | North Traps: Predicted optical properties. | 37 |
| Table 2-7: | Rolling Grounds: Predicted optical properties. | 39 |
| Table 2-8: | Project Reef: Predicted optical properties. | 41 |
| Table 2-9: | Source A North 20: Predicted optical properties. | 43 |

Figures

| | | |
|-------------|---|----|
| Figure 2-1: | Descriptive transects to show optical effects. | 9 |
| Figure 2-2: | Modelled euphotic zone depth. | 11 |
| Figure 2-3: | Modelled reduction in median euphotic zone depth (%). | 12 |
| Figure 2-4: | Mining at site A: Modelled euphotic zone depth along descriptive transects. | 13 |
| Figure 2-5: | Mining at site B: Modelled euphotic zone depth along descriptive transects. | 14 |
| Figure 2-6: | Modelled midwater horizontal visibility. | 16 |

| | | |
|--------------|--|----|
| Figure 2-7: | Modelled change in midwater horizontal visibility. | 17 |
| Figure 2-16: | Modelled water column light. | 20 |
| Figure 2-17: | Modelled change in water column light. | 21 |
| Figure 2-18: | Predicted effect of proposed mining on light at the seabed. | 23 |
| Figure 2-19: | Spatial distribution of mean light at the seabed. | 24 |
| Figure 2-20: | Spatial distribution of the modelled change in light at the seabed (%). | 25 |
| Figure 2-8: | Source A to Whanganui 20: Predicted effects of mining on cumulative distribution of near bed visibility and euphotic zone depth. | 28 |
| Figure 2-9. | Graham Bank: Predicted effects of mining on cumulative distribution of near bed visibility and euphotic zone depth. | 30 |
| Figure 2-10. | The Crack 1: Predicted effects of mining on cumulative distribution of near bed visibility and euphotic zone depth. | 32 |
| Figure 2-11. | The Crack 2: Predicted effects of mining on cumulative distribution of near bed visibility and euphotic zone depth. | 34 |
| Figure 2-12. | North Traps: Predicted effects of mining on cumulative distribution of near bed visibility and euphotic zone depth. | 36 |
| Figure 2-13. | Rolling Grounds: Predicted effects of mining on cumulative distribution of near bed visibility and euphotic zone depth. | 38 |
| Figure 2-14. | Project Reef: Predicted effects of mining on cumulative distribution of near bed visibility and euphotic zone depth. | 40 |
| Figure 2-15. | Source A North 20: Predicted effects of mining on cumulative distribution of near bed visibility and euphotic zone depth. | 42 |

Executive summary

Trans-Tasman Resources Ltd (TTR) propose to mine iron-sands in the South Taranaki Bight (STB) region. These activities will release sediment into the water column which will affect the optical properties¹ in some areas and at some times. This report summarises new “worst case” simulations of the optical effects of the proposed mining as requested by the Decision Making Committee (DMC) of the Environmental Protection Authority (EPA) in March 2017. The new results are compared with those from the “baseline” simulations as presented in Pinkerton & Gall (2015). The optical effects of the proposed mining at eight specific sites in the STB are also summarised. Revised videos of simulated movements of the plume of sediment discharged at over two years have also been produced and are provided with this report.

The main conclusions are:

1. Predicted optical effects in the new simulations are qualitatively similar to those from Pinkerton & Gall (2015), but quantitatively greater. Averaged across the sediment model domain, optical effects that are relevant to estimating effects on primary productivity were 44% greater in the new simulations than estimated using the models summarised in Pinkerton & Gall (2015). This considered effects of mining on mean light in the water column, mean light at the seabed, and the number of days per year when seabed light was greater than two ecologically-relevant limits.
2. Average light in the water column averaged over the domain of the sediment model is predicted to be reduced by only a small amount: 2.9% (mine A, was 1.9%) and by 2.4% (mine B, was 1.6%). Reductions in water column light are predicted to occur predominantly to the east of the mining site due to the sediment plume often moving in this direction.
3. The total amount of light received by the seabed in the domain of the sediment model is predicted to reduce by 30% (site A, was 23%) and 21% (site B, was 15%), and this reduction will primarily affect the area east of the proposed mining area.
4. On average, optical effects of mining at the selected eight stations are 41% greater in the new simulations than estimated using the models summarised in Pinkerton & Gall (2015). This considers four optical effects: horizontal visibility (midwater, seabed), number of high visibility days per year (in midwater and at seabed), euphotic zone depth, and number of days per year with >1% light at the seabed. The predicted effects are 2.2 times greater due to mining at site A than mining at site B.

¹ “Optical properties” are characteristics such as water colour and clarity. These are ecologically relevant because light availability affects primary productivity (how fast algae can grow in the water column and on the seabed). These algae are the base of most marine food-webs.

1 Introduction

1.1 TTR iron-sand mining proposal

Trans-Tasman Resources Ltd. (TTR) propose to mine iron-sands within the South Taranaki Bight (STB) region. These activities will release sediment into the water column. The probable spatial patterns of suspended sediment concentrations (SSC) from a mining plume have been simulated, using a sediment transport model for a range of size classes and driven by the expected mining operations. There are two main types of effects from changes in water column SSC: (1) ‘Mass Effects’ (smothering or disruptive effects of suspended sediment on organisms); and (2) ‘Optical Effects’. Pinkerton & Gall (2015) summarised modelling to estimate the optical effects of the sediment discharge. Cahoon et al. (2015) assessed the effects of these changes to optical properties on primary production and energy flow to the benthos.

1.2 Worst-case simulations

As part of the 2017 application for consent under the New Zealand EEZ Act, the Decision Making Committee (DMC) of the Environmental Protection Authority (EPA) requested further “worst case” simulations of suspended sediment discharges.

Macdonald & Hadfield (2017) carried out new “worst-case” simulations of sediment transport in the STB region in March 2017. They report:

“This worst case scenario differs from previous simulations as it uses a time-varying source term. The new source term assumes varying fines content in the material to be mined and also takes into account increased sediment release during mound building and an increase in sediment release during periods of high waves. The downtime for the mining operations has also been increased from 20% to 29% following new information on operational restrictions from TTR.” (Macdonald & Hadfield, 2017)

For more details of the “worst-case” hydrodynamic simulations, please see Macdonald & Hadfield (2017).

Based on these new simulations of SSC (Macdonald & Hadfield, 2017), the present report uses the approach of Pinkerton & Gall (2015) to assess the optical effects. These are relevant to estimating “worst-case” effects on primary production following the approach of Cahoon et al. (2015) but this analysis is not included here – this is strictly an “optical effects” analysis.

Optical effects at eight specific locations in the STB were also requested by the DMC and are included here. Although most of these stations were not included in Pinkerton & Gall (2015), the original simulations were used to estimate optical effects at all eight stations to enable comparison with the present worst-case scenario.

1.3 Mining at site A and site B

The hydrodynamic model (Macdonald & Hadfield, 2017) is run three times: (1) background (no mining); (2) mining at site A (inner limit of proposed mining) and site B (outer limit of proposed mining). In each case, two years are simulated to enable information consistent with natural variability to be developed. In reality, the location of mining will change over time, so that the “mine A” and “mine B” scenarios may be considered as “bracketing” the likely optical effects of mining.

2 Predicted optical effects

2.1 Descriptive transects

Euphotic zone depth and underwater visibility were extracted on three descriptive transects (Figure 2-1): (1) nearshore; (2) south-north through the proposed mining area; (3) west-east approximately through the main axis of the plume. The results are based on statistics derived from the 1460 model realisations of the domain, covering a period of two years at 12 hourly intervals. The model is run three times: (1) background (no mining); (2) mining at site A (inner limit of proposed mining) and site B (outer limit of proposed mining).

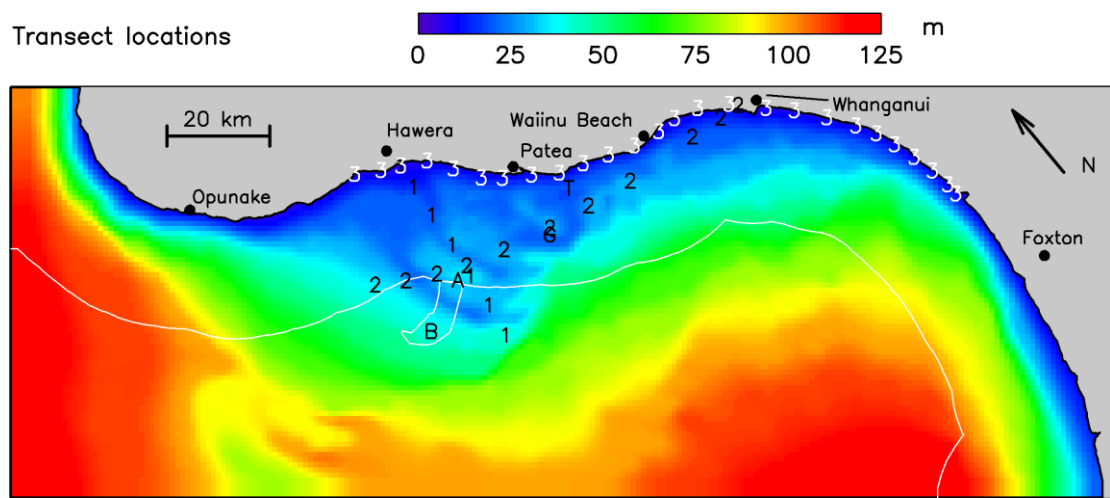


Figure 2-1: Descriptive transects to show optical effects. The three descriptive optical transects are: (1) south to north, "1" black; (2) west to east, "2" black; (3) alongshore, "3" white. The west-east and south-north transects pass through the proposed area of mining and are approximately aligned along and across the main axis of the modelled sediment plume. Background colour shows water depth. Mining site A is labelled "A", mining site B is labelled "B", Graham Bank is labelled "G" and the Traps is labelled "T".

2.2 Euphotic zone depth

Modelling of mining activities at release location a, causes a reduction in euphotic zone depth (z_{eu}). The euphotic zone depth is the depth at which the downwelling irradiance has fallen to 1% of its surface value. This is often taken as indicative of the zone within which primary production occurs by phytoplankton in the water column and microphytobenthos on the seabed. A reduction in the euphotic zone depth implies less light is available for primary production.

Results are shown in Figure 2-2, Figure 2-3, Figure 2-4 and Figure 2-5. Overall, euphotic zone depths are greater over deeper water, further away from the coast, and smaller over shallower water and near the coast (Figure 2-2a). This is a result of greater concentrations of suspended sediment, CDOM and phytoplankton in shallower water. Mining leads to increased suspended sediment in the water column which has a shading effect and leads to lower euphotic zone depths. The degree to which euphotic zone depth is reduced depends on how the suspended sediment plume behaves – its movement by the currents, the mixing (dispersion) of the material in the water, and the settling of the sediment to the seabed. The movement of the plume is most commonly in an easterly direction from the mining site. Because there is substantial variability in how the suspended sediment plume behaves, both in terms of the direction it moves and how rapidly the sediment disperses or settles, the optical effect reduces with distance away from the mining site (compare brown and blue median lines in Figure 2-4 and Figure 2-5).

One important result from this modelling is that the mining reduces how much light reaches the seabed in the area of the west-east and south-north transects. Note that the blue lines in Figure 2-4 (median euphotic zone depths with no mining) are much closer to the depth of the seabed (black lines) in the background case compared to when mining is present. With mining at site A or site B, the median euphotic zone depths (brown lines) are considerably shallower than the seabed. This change is less with mining at site B compared to site A because this mining site is further away from the west-east and south-north transects than site A.

In contrast to the effects of mining on euphotic zone depth along the west-east and south-north transects, the mining is predicted to have only a very small effect on euphotic zone depth along the alongshore transect. For the alongshore transect, the brown and blue median lines are indistinguishable in Figure 2-4, Figure 2-5, and the distributions show only a small change. The outliers of high euphotic zone depth on the alongshore transect (red dots in lower panels of these figures) indicate that clear blue water sometime reaches the coast and that this is essentially unaffected by the mining.

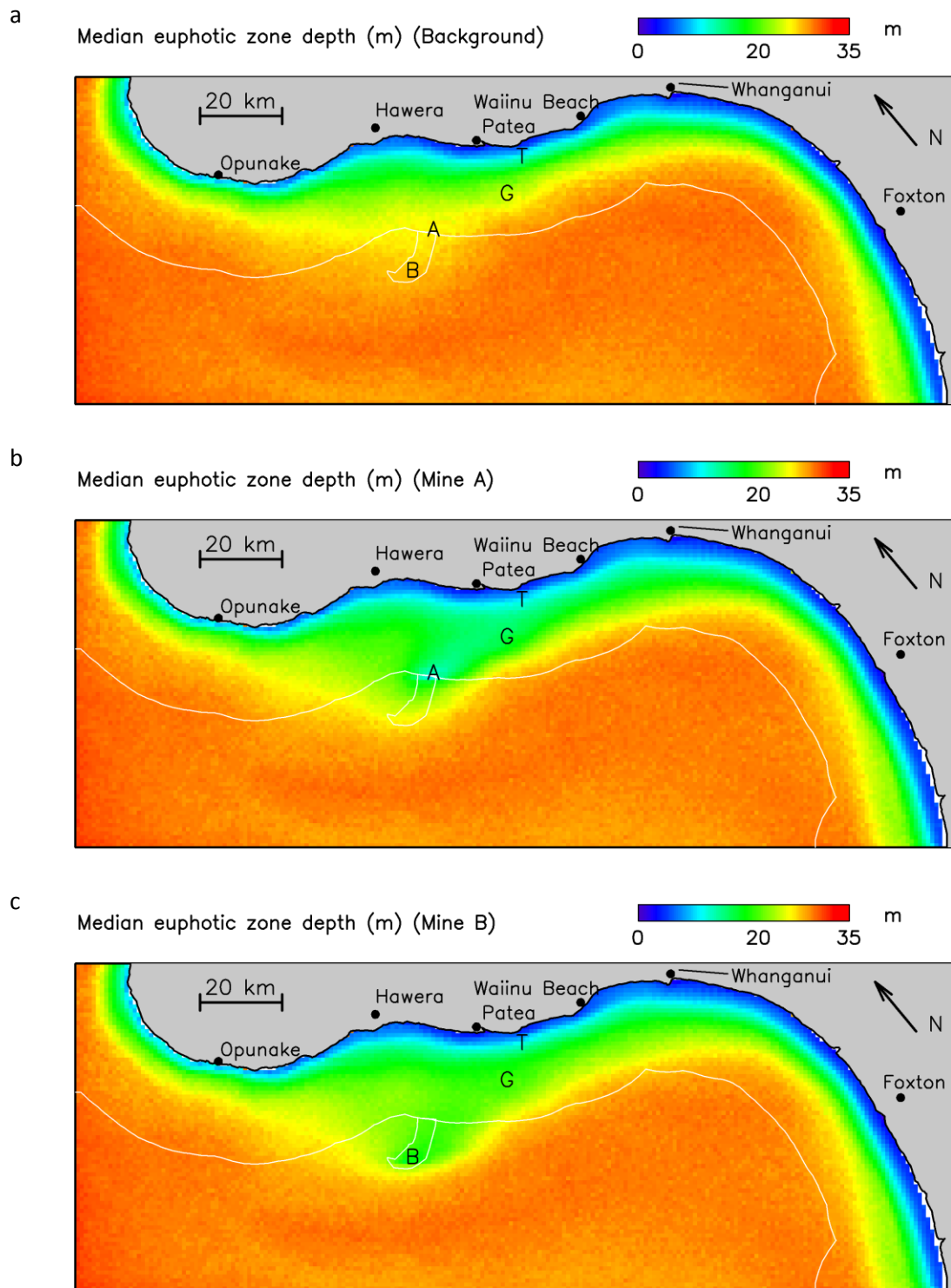
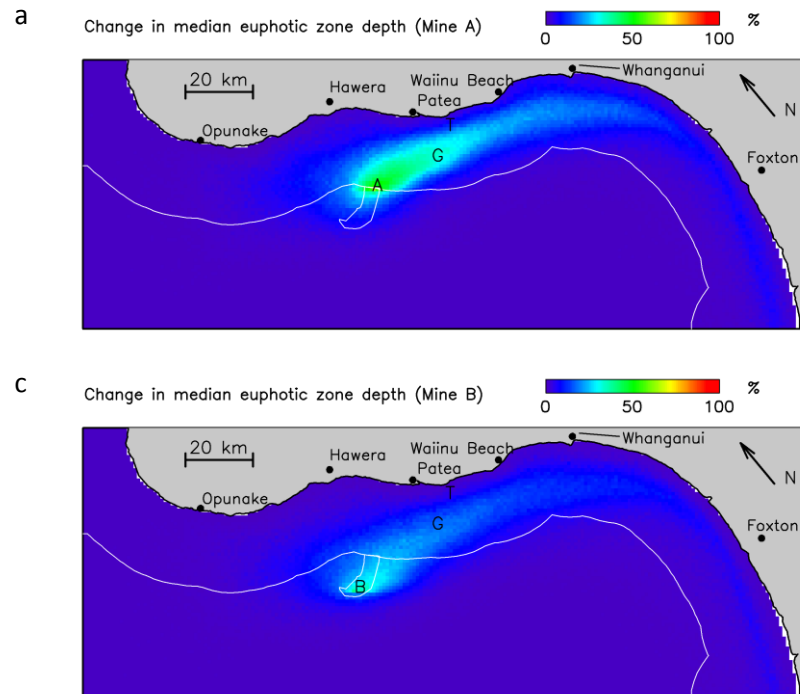


Figure 2-2: Modelled euphotic zone depth. Modelled median euphotic zone depth under **a:** background (no mining); **b:** mining at site A (labelled “A”); **c:** mining at site B (labelled “B”). Graham Bank is labelled “G” and the Traps is labelled “T”. “Rate 1” means the full proposed mining rate.

This study



Pinkerton & Gall (2015)

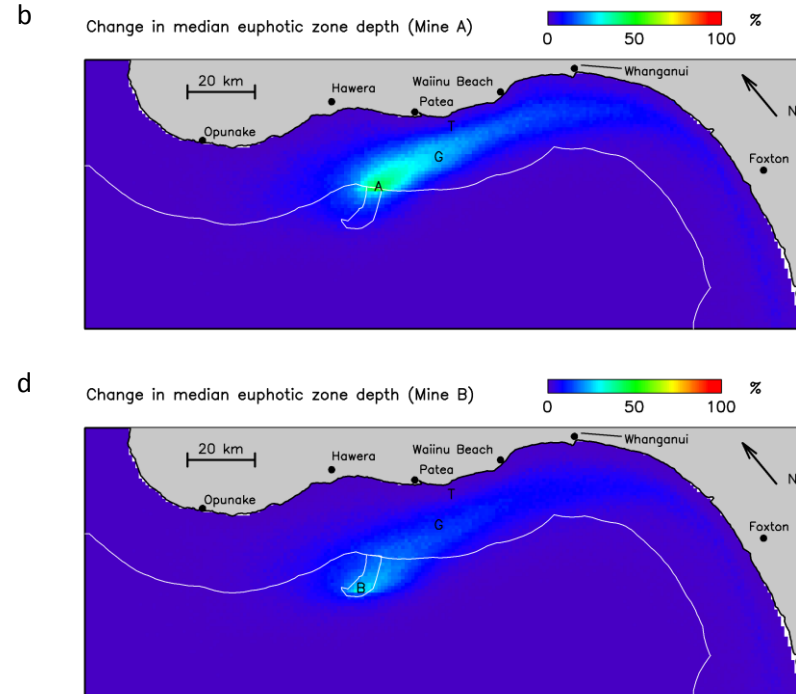


Figure 2-3: Modelled reduction in median euphotic zone depth (%). Modelled percentage reduction in median euphotic zone depth under **a, b**: mining at site A (labelled “A”); **c, d**: mining at site B (labelled “B”). New simulations are shown in the left column (a, c) and those from Pinkerton & Gall (2015) in the right column (b, d). Graham Bank is labelled “G” and the Traps is labelled “T”.

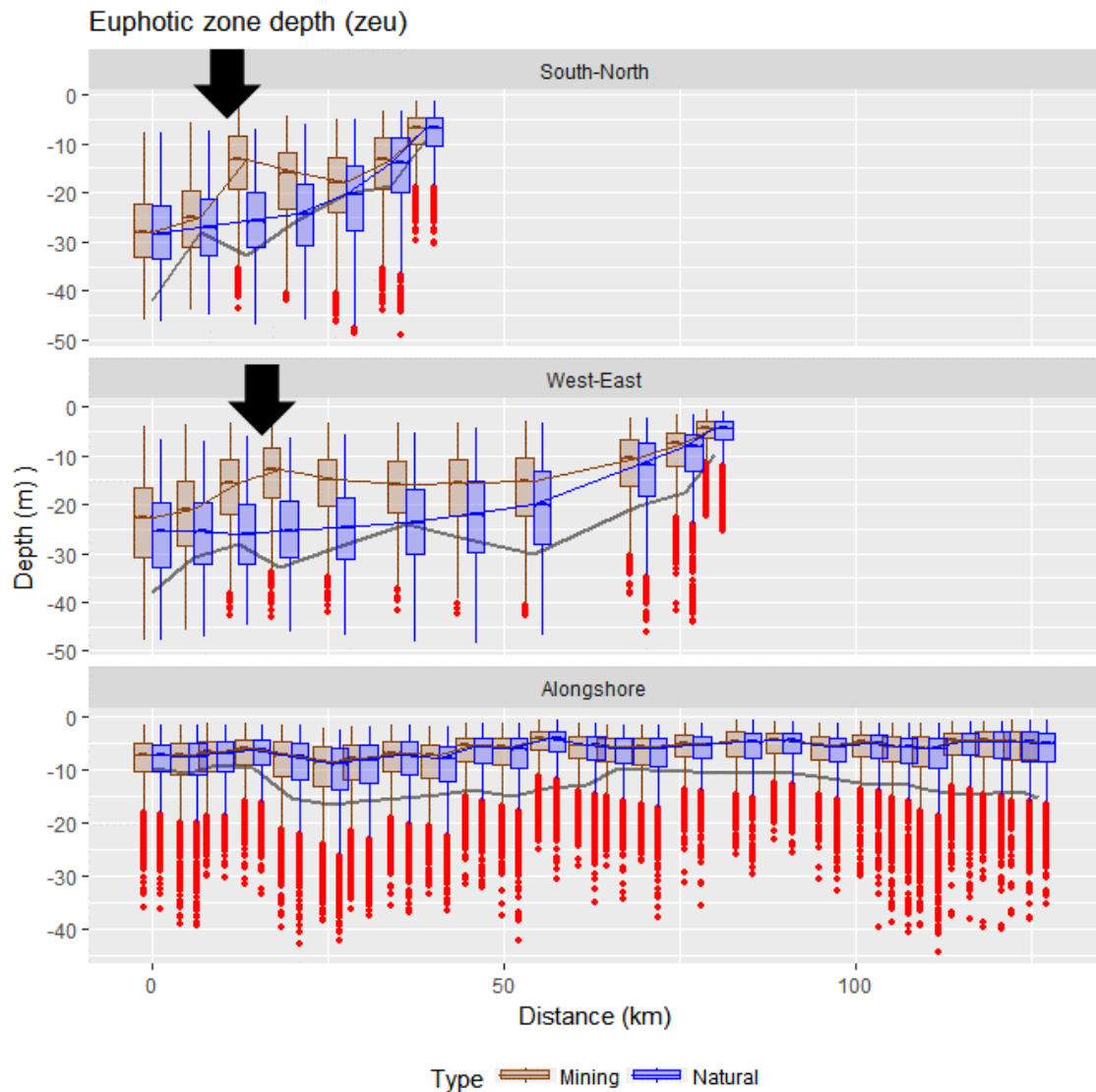


Figure 2-4: Mining at site A: Modelled euphotic zone depth along descriptive transects. Modelled euphotic zone depth under background and mining conditions along transects show Figure 2-1. Boxplots enclose 50% of the data (25th to 75th percentiles derived from the 1460 model runs) around the median (central lines in boxes, joined with brown and blue lines). Whiskers extend beyond the quartiles by 1.5 times the interquartile-range or to the maximum/minimum data values. Red symbols are “outliers” beyond the range of the whiskers (McGill et al., 1978). The sea-floor is indicated by the black line. The black arrows indicate the location of mine site A on the south-north and west-east transects.

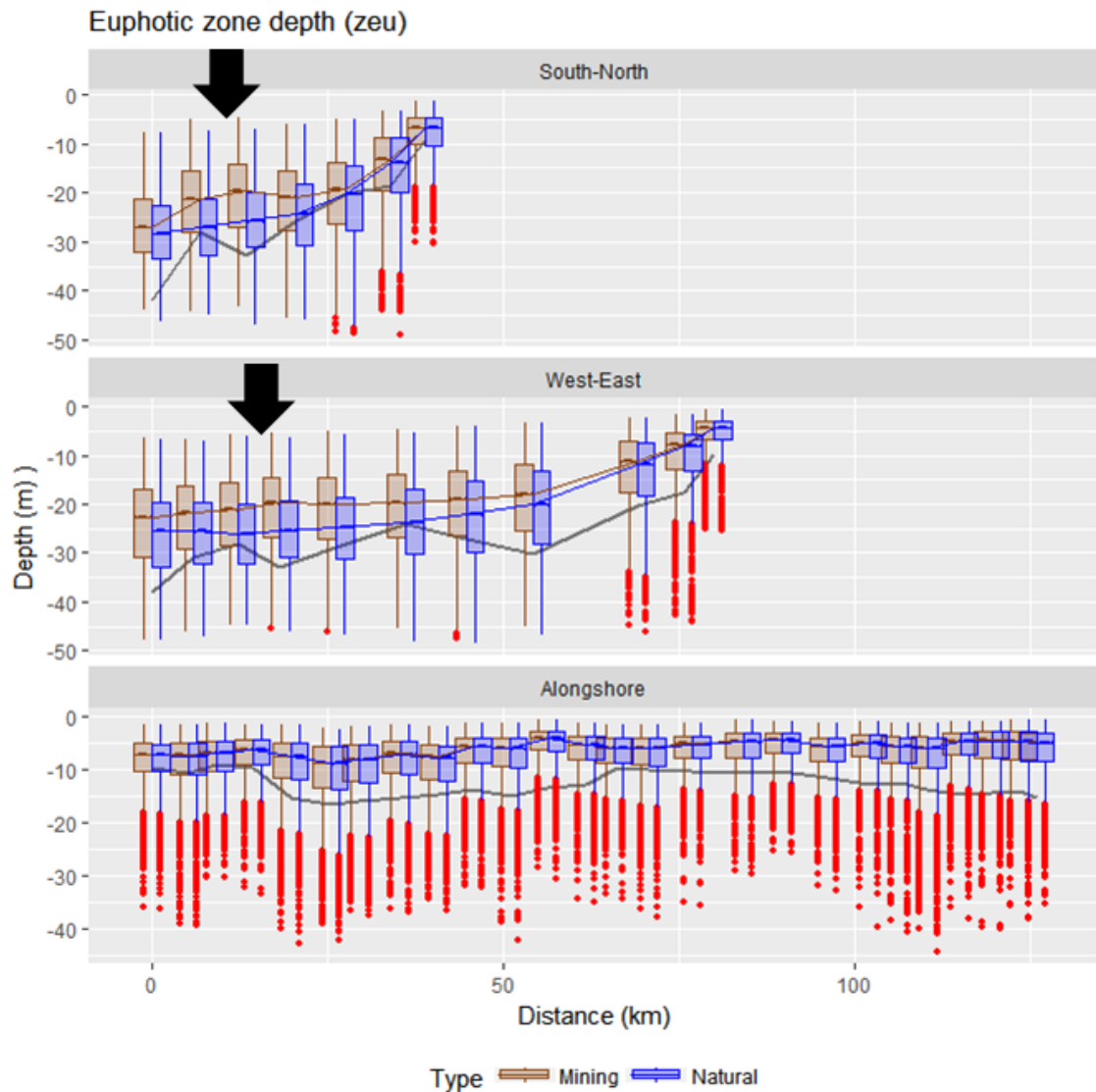


Figure 2-5: Mining at site B: Modelled euphotic zone depth along descriptive transects. As for Figure 2-4 but for mining at site B. The black arrows indicate the approximate location of mine site B on the south-north and west-east transects.

2.3 Horizontal visibility (Black disk distance)

Low horizontal visibilities in the midwater tend to be found near the coast with higher visibilities beyond about 10 km from the coast (Figure 2-6). Patterns in changes to median horizontal visibility in the midwater due to mining at site A and site B follow changes to euphotic zone depth (Figure 2-7). These main patterns are:

- (1) There are substantial reductions in midwater visibility due to mining close to the mining site (maximum changes of 83% mining at site A; 66% mining at site B). In Pinkerton & Gall (2015), these maximum reductions in midwater visibility were 77% and 61% respectively. As in Pinkerton & Gall (2015), these predicted effects of mining on horizontal visibility decrease with distance from the mining site (Figure 2-7).
- (2) Reductions in midwater visibility at a given time depend on the movement of the plume and how rapidly the sediment discharged by the mining is mixed and sinks out of the water column. The predominant area affected is a region around the mining site with a tail stretching to the east.
- (3) There are likely to be only very small effects of mining on midwater visibility on the alongshore transect.

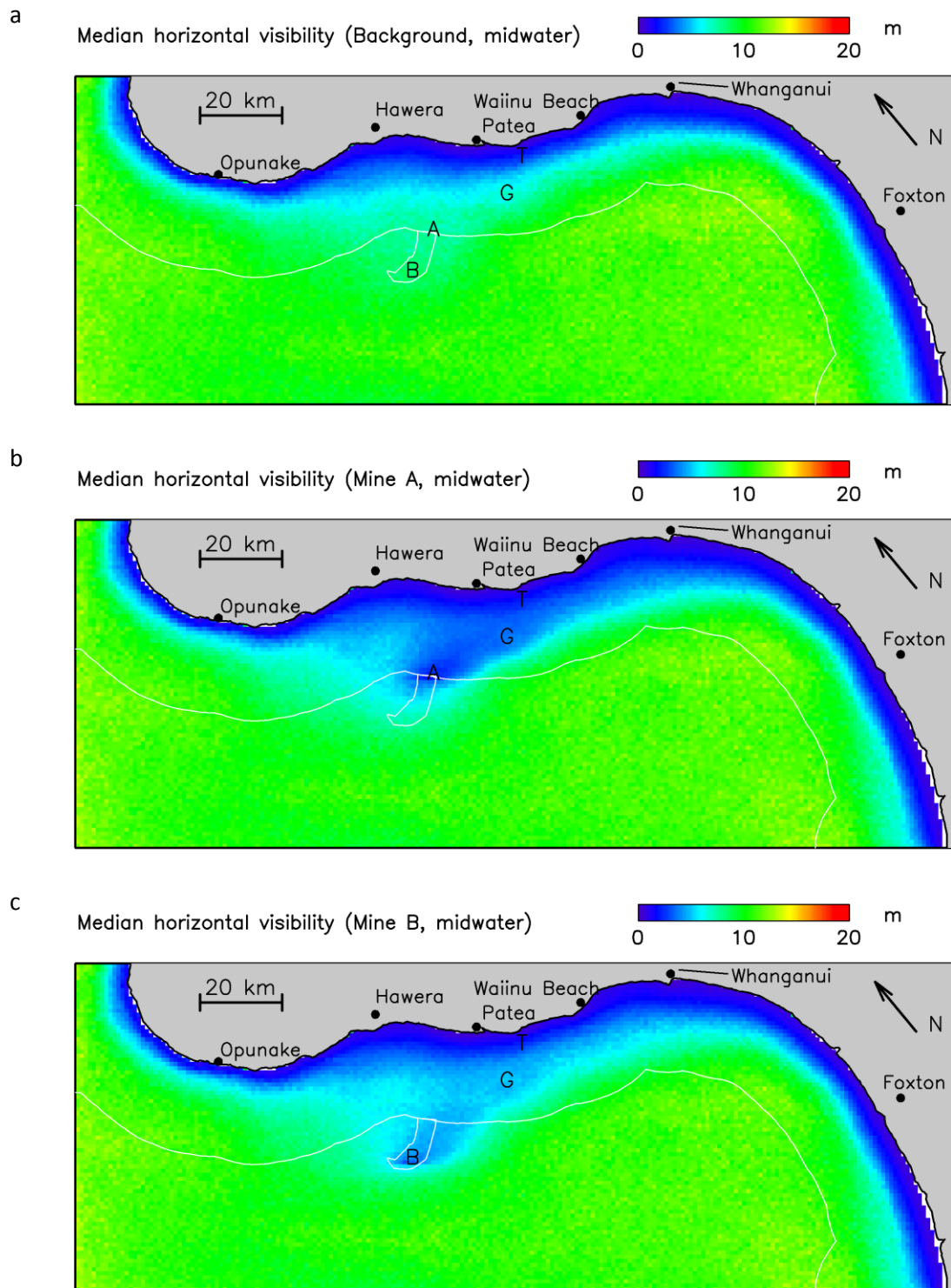
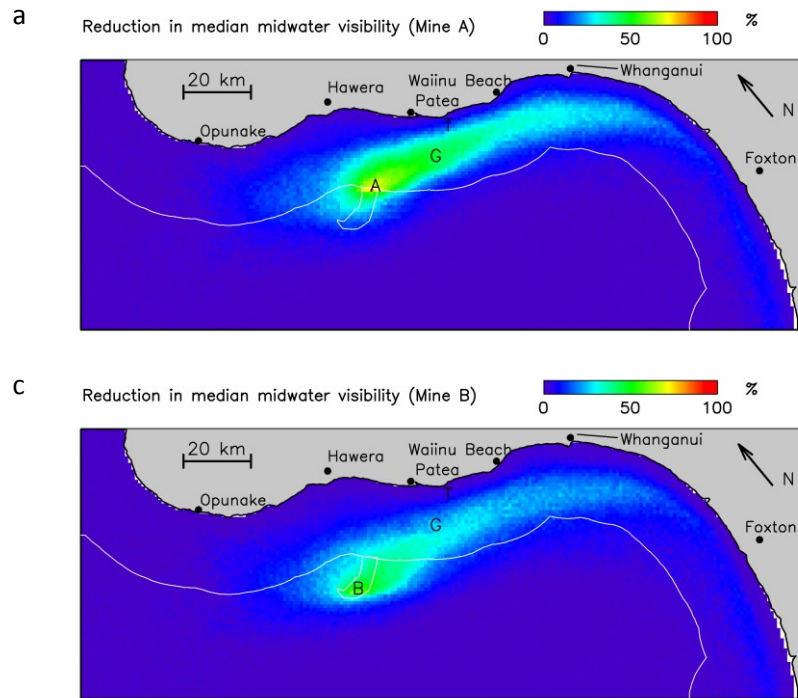


Figure 2-6: Modelled midwater horizontal visibility. Modelled median midwater horizontal visibility under **a**: background (no mining); **b**: mining at site A (labelled “A”); **c**: mining at site B (labelled “B”). Graham Bank is labelled “G” and the Traps is labelled “T”.

This study



Pinkerton & Gall (2015)

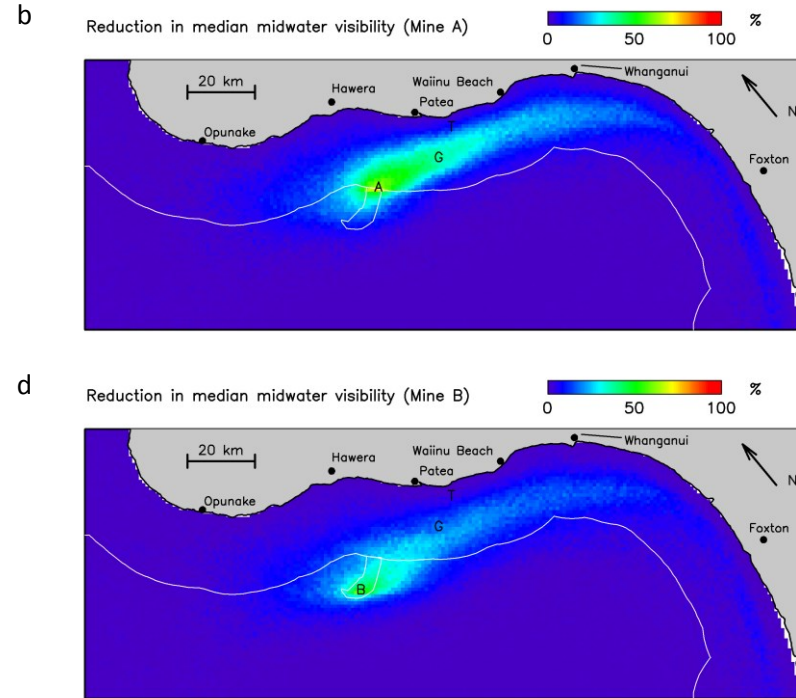


Figure 2-7: Modelled change in midwater horizontal visibility. Modelled reduction in median horizontal visibility under **a, b**: mining at site A (labelled “A”); **c, d**: mining at site B (labelled “B”). New simulations are shown in the left column (a, c) and those from Pinkerton & Gall (2015) in the right column (b, d). Graham Bank is labelled “G” and the Traps is labelled “T”.

2.4 Water colour

The optical modelling also estimated the colour of the sea seen by an observer looking vertically downwards at the sea surface for three cases: no mining (background), with mining at site A and with mining at site B. The images were produced for each of the 1460 time steps of the model covering the two year simulation at 12 hour resolution. These data were used to produce revised videos of the predicted change in apparent water colour. These videos are useful for context as they show variations in the background sediment in the STB and the predicted appearance and behaviour of the mining-generated sediment plume over the same period.

2.5 Water column light intensity

Changes to the intensity of light in the water column has the potential to affect the primary productivity of phytoplankton (Kirk, 2011; Cahoon et al., 2015). Changes in colour (spectral signatures) of light could affect phytoplankton growth but is likely to be less important than changes to the intensity of light in the water column (Falkowski & Raven, 1997). Hence, based on the optical modelling, we calculated the change in light in the water column due to mining. For each 1 km² cell in the SMD for each model realisation over the two years of model simulations, we calculated the integrated water column light intensity as a proportion of the surface light based on the modelled euphotic zone depth and total water depth (Pinkerton & Gall, 2015). Where the water depth is greater than the euphotic depth, this is within 1% of water column light integrated over just the photic zone. The background values of water column light are shown in Figure 2-8a. Water column light generally increases with distance away from the coast because suspended sediment, CDOM and elevated phytoplankton concentrations near the coast reduce the penetration of light into the water, and because the water is shallower further offshore.

The effects of mining on water column light are summarised in Table 2-1 and shown spatially in Figure 2-8 and Figure 2-9.

There are large reductions in light in the water column only very close to the location of mining, with maximum reductions of 32–52%, depending a little on where the mining takes place (site A or site B). Note that this maximum depends on the resolution of the modelling – cells smaller than the 1 km used here would give a higher maximum changes and vice versa. The mean change in water column light averaged over a large region is a more reliable measure of the predicted effect of mining on primary production in the water column. The mean change in water column light due to mining over the SMD were small: -2.9% (mining at site A) and -2.4% (mining at site B). These results are relevant to considering the effect of the proposed mining on primary productivity in the STB (cf. Cahoon et al., 2015).

Table 2-1: Modelled effect of mining on water column light. The change in mean water column light due to mining is used to estimate the effect of mining on primary production by phytoplankton at the scale of the Sediment Model Domain (SMD) (see Cahoon et al., 2015). For comparison, results based on the optical modelling of Pinkerton & Gall (2015) are shown and shaded grey. * Note that the maximum change depends on the spatial resolution of the modelling.

| Measure of water column light | Present study | | | Pinkerton & Gall (2015) | | |
|---|---------------|--------|--------|-------------------------|--------|--------|
| | Back-ground | Mine A | Mine B | Back-ground | Mine A | Mine B |
| Mean water column light as a proportion of surface light over SMD (m) | 5.5 | 5.4 | 5.4 | 5.5 | 5.4 | 5.4 |
| Median change over SMD (%) | | -0.4 | -0.6 | | -0.3 | -0.4 |
| Maximum change (%) * | | -51.9 | -31.6 | | -45.5 | -26.6 |
| Mean change over SMD (%) | | -2.9 | -2.4 | | -1.9 | -1.6 |

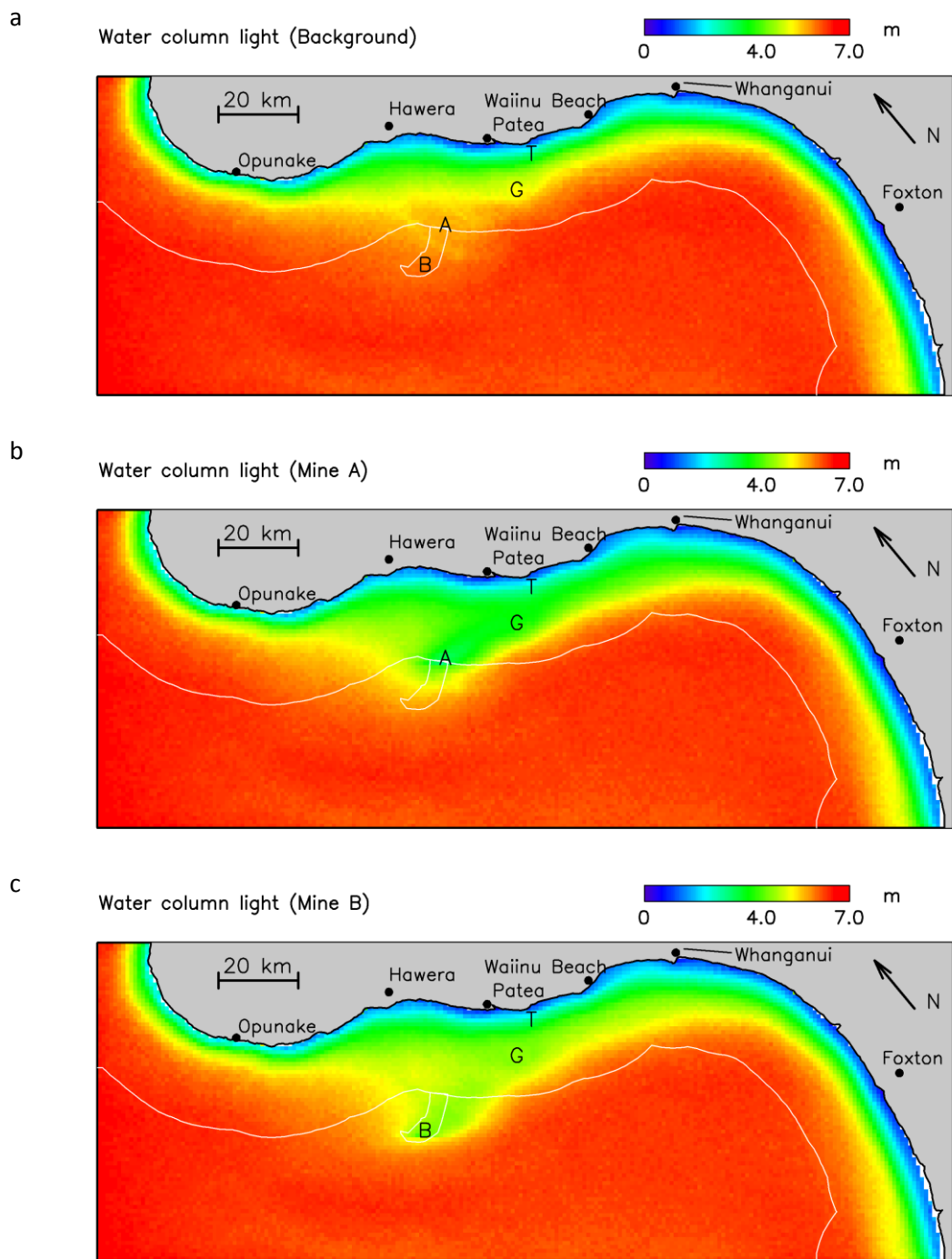


Figure 2-8: Modelled water column light. Modelled water column light under **a**: background (no mining); **b**: mining at site A (labelled “A”); **c**: mining at site B (labelled “B”). Graham Bank is labelled “G” and the Traps is labelled “T”.

This study

Pinkerton & Gall (2015)

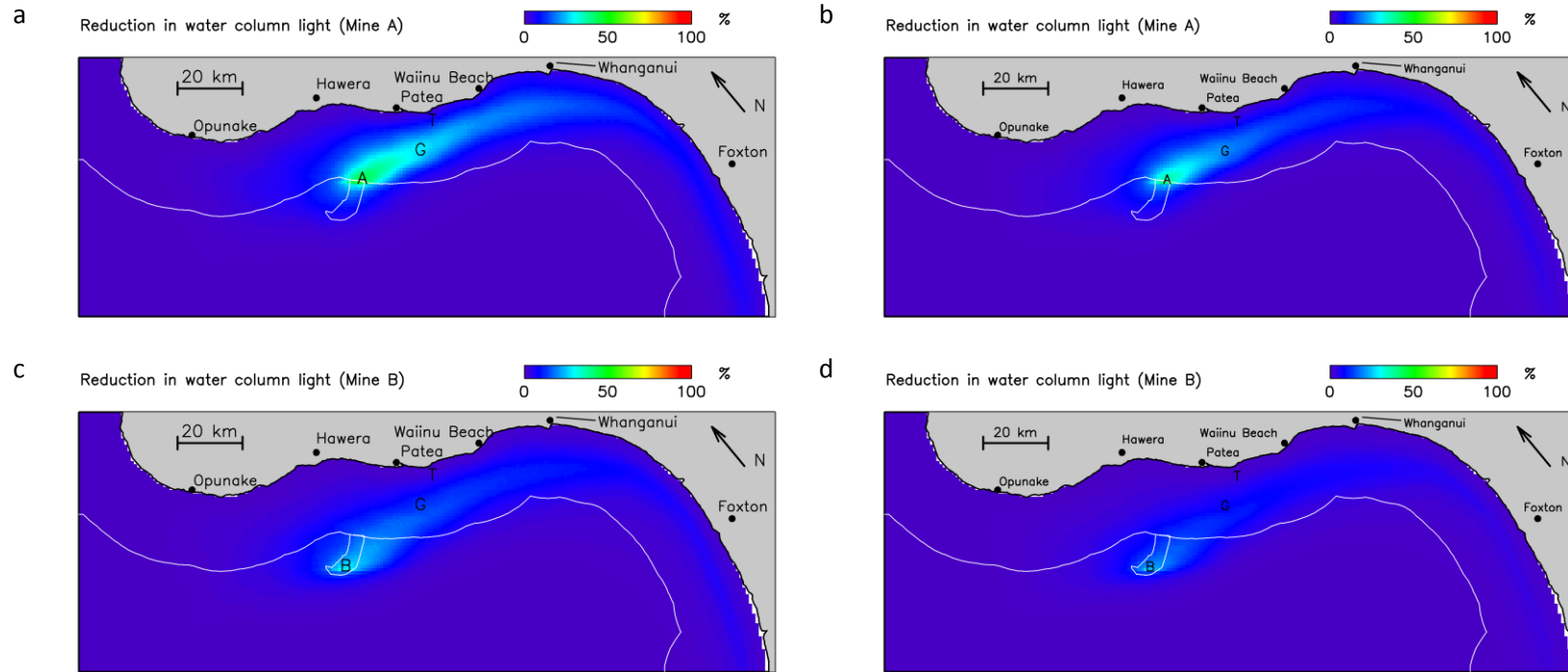


Figure 2-9: Modelled change in water column light. Modelled changes in water column light as a proportion of background under **a, b**: mining at site A (labelled “A”); **c, d**: mining at site B (labelled “B”). New simulations are shown in the left column (a, c) and those from Pinkerton & Gall (2015) in the right column (b, d). Graham Bank is labelled “G” and the Traps is labelled “T”.

2.6 Light at the seabed

Light reaching the seabed can be used by benthic algae for primary production. Benthic algae includes macroalgae (“seaweed”) and benthic microalgae (“microphytobenthos”, MPB; Cahoon, 2014; Huettel et al., 2014). The consequences of reduced light at the seabed for benthic PP depend on what macroalgae and MPB are present, what reductions in light at the seabed occur, and the sensitivity to benthic PP on light availability rather than other factors; these are considered in Cahoon et al. (2015).

The amount of light reaching the seabed was modelled before and after mining over the SMD as described in Pinkerton & Gall (2015). Results are summarised in Figure 2-10 and Table 2-2; maps are given Figure 2-11 and Figure 2-12.

The average proportions of the seabed in the SMD with mean light intensity greater than two limits (0.04 and 0.4 mol/m²/d) was estimated to be 28% (3775 km²) and 11% (1478 km²) respectively. These areas are predicted to reduce to 25–26% and 9% (respectively) due to mining (Figure 2-10). The effect of mining is to reduce the amount of light reaching the seabed because the sediment plume absorbs and backscatters some light in the water column before it reaches the seabed.

There are predicted to be large reductions in light at the seabed close to the location of mining, with maximum reductions of 87–92%, depending on where the mining takes place (site A or site B). Note that this maximum reduction depends on the resolution of the modelling – smaller cells (higher resolution modelling) would give a higher maximum changes and vice versa. The maximum change should hence not be over-interpreted in terms of its ecological significance, and the mean change in total light at the seabed averaged over a large region (the SMD) is a more reliable measure of the predicted effect of mining on benthic algae. The annual-average light at the seabed within the area of the SMD is predicted to reduce by 30% (mining at site A) and 21% (mining at site B).

This reduction reflects the fact that for much of the time the plume of fine sediment passes over relatively shallow sea floor which would otherwise be relatively well lit. Most of the SMD is deep and/or overlain by turbid water, receives little seabed light and would be little affected by the mining.

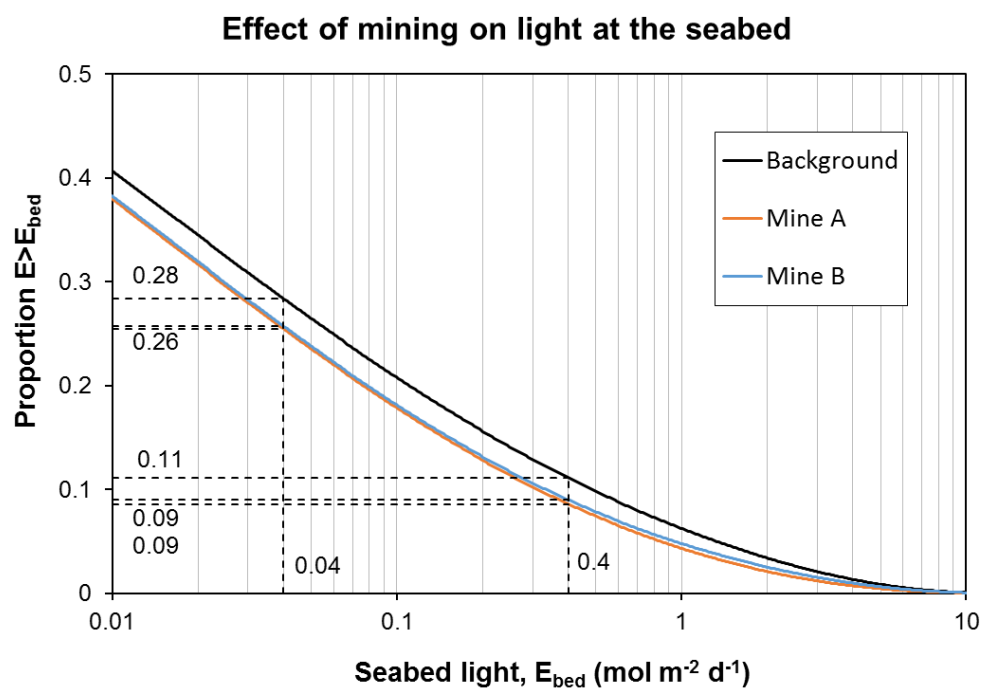


Figure 2-10: Predicted effect of proposed mining on light at the seabed. The y-axis shows the proportion of the seabed area of the Sediment Model Domain (SMD; part of the South Taranaki Bight) that has more than the amount of light (E_{bed}) shown on the x-axis. The change to the amount of area receiving more than $0.04 \text{ mol/m}^2/\text{d}$ is 9–10%, and the change to the amount of area receiving more than $0.4 \text{ mol/m}^2/\text{d}$ is 19–23%, all calculated over the two years of model simulations.

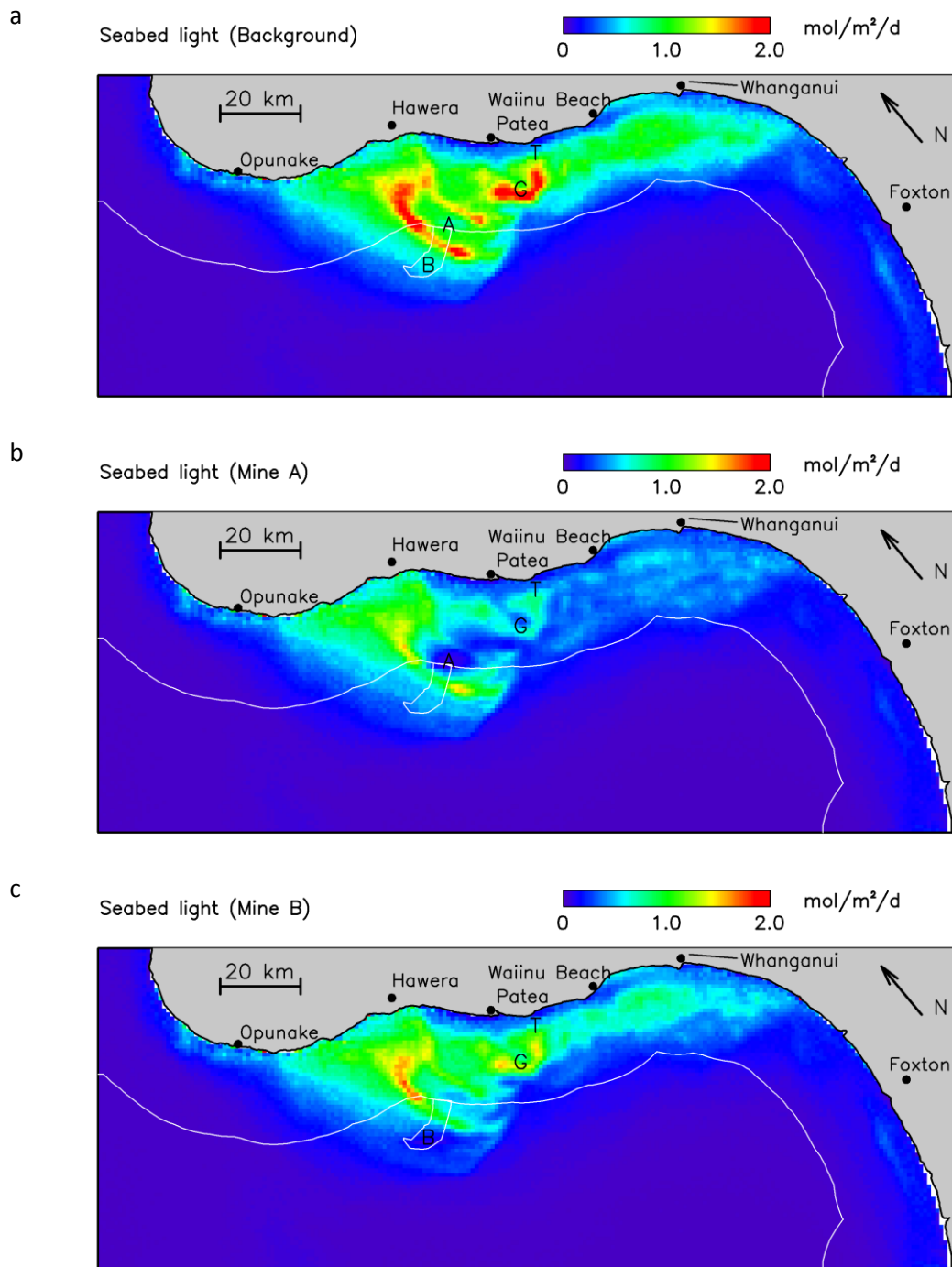
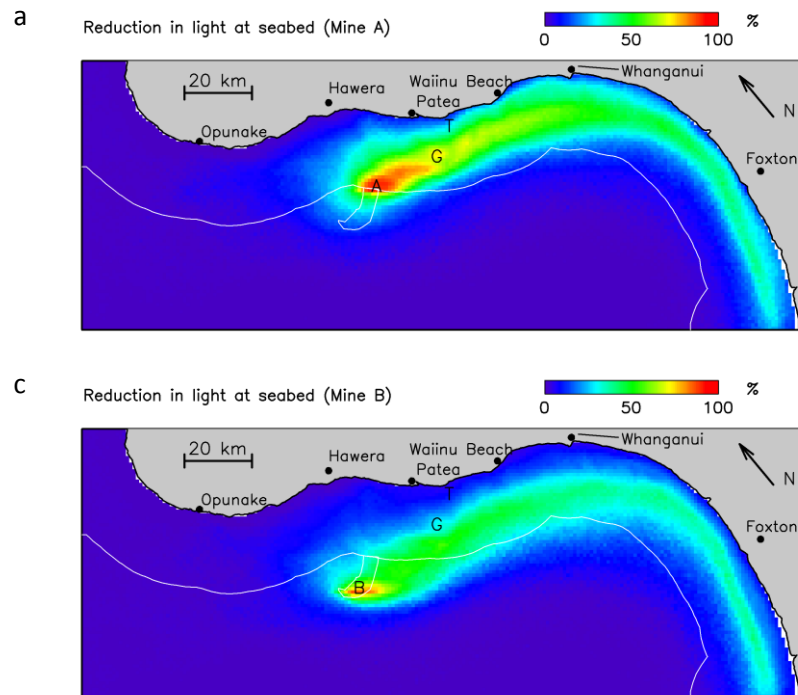


Figure 2-11: Spatial distribution of mean light at the seabed. Modelled mean seabed light (mol/m²/d) under **a**: background (no mining); **b**: mining at site A (labelled “A”); **c**: mining at site B (labelled “B”). Graham Bank is labelled “G” and the Traps is labelled “T”.

This study



Pinkerton & Gall (2015)

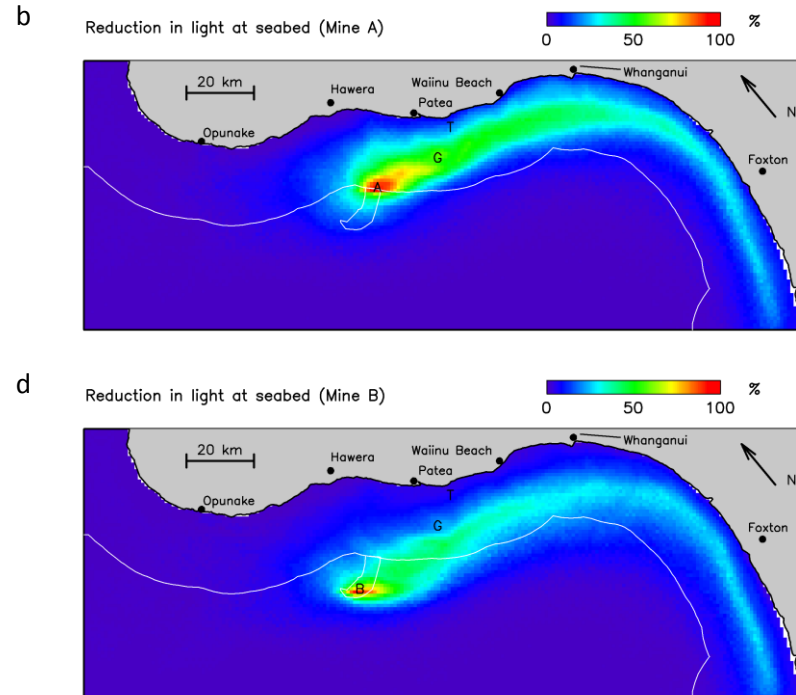


Figure 2-12: Spatial distribution of the modelled change in light at the seabed (%). Modelled changes in sea-bed light as a proportion of background under **a, b**: mining at site A (labelled “A”); **c, d**: mining at site B (labelled “B”). New simulations are shown in the left column (a, c) and those from Pinkerton & Gall (2015) in the right column (b, d). Graham Bank is labelled “G” and the Traps is labelled “T”.

Table 2-2: Predicted changes to optical properties. Optical properties for estimating effects on primary productivity (PP) by microphytobenthos (MPB) in the Sediment Model Domain (SMD) part of South Taranaki Bight (STB). For comparison, results based on the optical modelling of Pinkerton & Gall (2015) are shown and shaded grey. * Note that highest point change identified is dependent on the spatial scale of the modelling.

| Parameter | Measure | Present study | | | Pinkerton & Gall (2015) | | |
|--|---|---------------|------------------|------------------|-------------------------|------------------|------------------|
| | | Background | Mining at site A | Mining at site B | Background | Mining at site A | Mining at site B |
| Prop seabed area with light >limit (mol/m ² /d) | Area with E>0.04 (% of SMD) | 28.4 | 25.5 | 25.7 | 28.6 | 26.6 | 26.9 |
| | Area with E>0.4 (% of SMD) | 11.1 | 8.6 | 9.0 | 11.2 | 9.4 | 9.7 |
| | Change in area with E>0.04 (%) | | -10.3 | -9.3 | | -6.8 | -6.0 |
| | Change in area with E>0.4 (%) | | -22.7 | -19.1 | | -16.5 | -13.8 |
| Light at the seabed | Mean total seabed light over SMD (Gmol/d) | 3.2 | 2.3 | 2.5 | 3.3 | 2.5 | 2.8 |
| | Change in mean total light at seabed over SMD (%) | | -30.0 | -21.0 | | -22.8 | -15.5 |
| | Highest point change in mean seabed light (%) | | -92.1 * | -87.1 * | | -95.1 * | -91.8 * |

2.7 Optical effects at selected stations

Model data were extracted to investigate the effects of mining at eight selected stations (Table 2-3, Figure 2-13). See Macdonald & Hadfield (2017) for more details on these stations. Results are summarised for euphotic zone depth and horizontal visibility near the seabed. The figures below show the cumulative distributions of the optical properties with no mining (background case, black lines) and with mining at site A (red lines) and at site B (blue lines). This type of cumulative distribution plot is used because it summarises the variability in the model information rather than just the median value. In these plots, the value of the optical property is shown on the x-axis and the y-axis shows the proportion of the time that the optical property was modelled to be less than this amount. The median value of the optical property is hence the value of x for which $y=0.5$. The plots also allow us to summarise the proportion of time that the optical property can be expected to be greater than a certain value. We are interested in the proportion of the time that the seabed receives more than 1% of light as this is likely to be indicative of the potential for benthic primary production. For horizontal visibility, we summarise how often horizontal visibility is more than 5 m – these are called “good visibility days” – and may indicate recreational amenity value (Pinkerton & Gall, 2015).

Table 2-3: Locations and approximate water depths at selected stations. The location of “Project Reef” station is not publically available.

| Site | Longitude °E | Latitude °S | Depth (m) |
|--------------------------|--------------|-------------|-----------|
| Source A to Whanganui 20 | 174.432 | 39.877 | 21.7 |
| Graham Bank | 174.419 | 39.892 | 22.0 |
| The Crack 1 | 174.250 | 39.820 | 27.2 |
| The Crack 2 | 174.300 | 39.850 | 27.5 |
| North Traps | 174.524 | 39.853 | 18.3 |
| Rolling Grounds | 174.373 | 39.958 | 49.3 |
| Project Reef | NA | NA | NA |
| Source A North 20 | 174.200 | 39.669 | 20.1 |

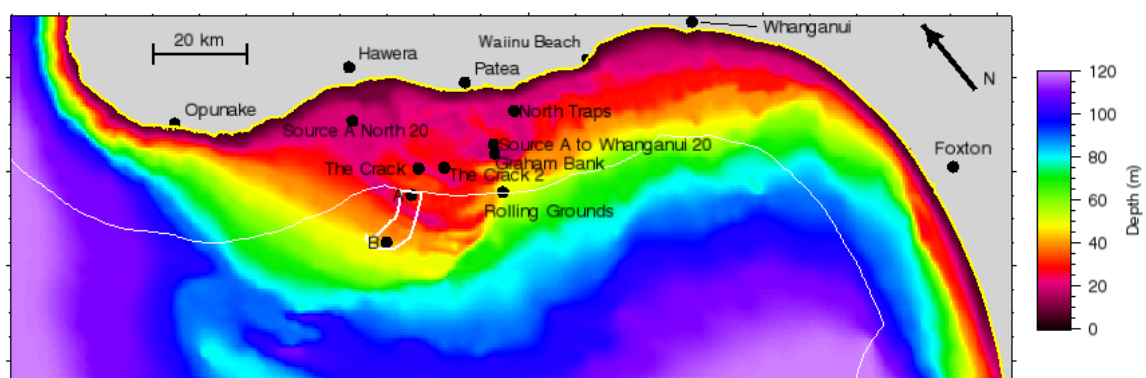


Figure 2-13: Stations of interest. The stations of interest are shown. Note that the Reef Project is not indicated on this figure as the stakeholder would prefer this location to remain hidden.

2.7.1 Source A to Whanganui 20: Predicted optical effects

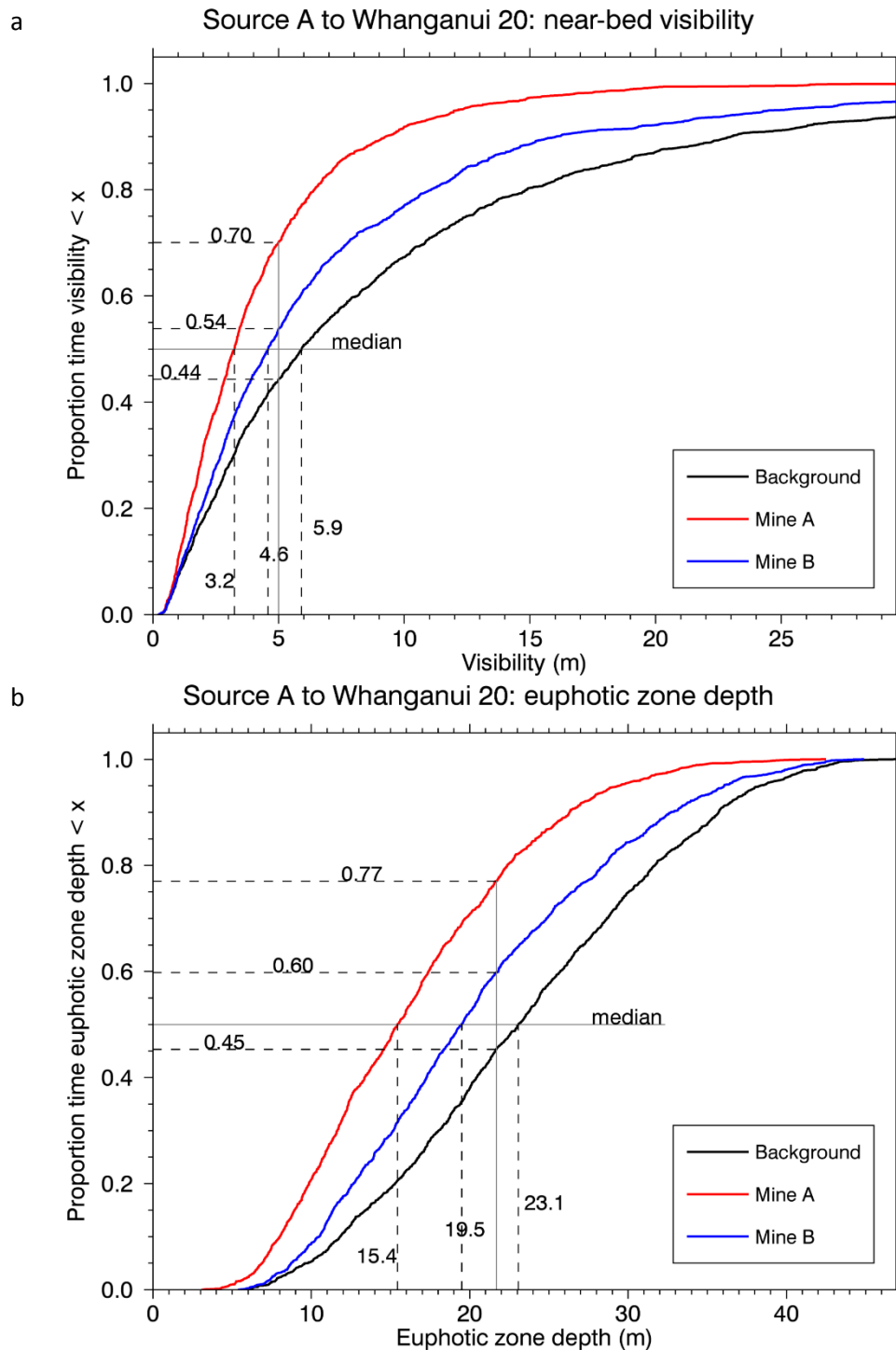


Figure 2-14: Source A to Whanganui 20: Predicted effects of mining on cumulative distribution of near bed visibility and euphotic zone depth. Background (no mining) – black; Mining at site A – red; Mining at site B – blue. Dashed lines show the median values and the proportions of time for which the euphotic zone depth is less than the depth of the seabed.

Table 2-4: Source A to Whanganui 20: Predicted optical properties. Predicted optical properties and their changes from background conditions if iron-sand recovery operations took place at the inner (Site A) or outer (Site B) end of the proposed mining area. For comparison, results based on the optical modelling of Pinkerton & Gall (2015) are shown and shaded grey.

| Metric | | Present study | | | Pinkerton & Gall (2015) | | |
|--------------------------------------|------------------------|---------------|--------|--------|-------------------------|--------|--------|
| | | Back-ground | Site A | Site B | Back-ground | Site A | Site B |
| Horizontal visibility | Median (midwater) (m) | 6.5 | 3.4 | 4.9 | 6.5 | 4.0 | 5.4 |
| | Median (seabed) (m) | 5.9 | 3.2 | 4.6 | 6.3 | 3.8 | 5.3 |
| | Change (midwater) (%) | | -47.1 | -24.6 | | -38.9 | -16.5 |
| | Change (seabed) (%) | | -45.3 | -22.6 | | -39.9 | -15.4 |
| High visibility days (days per year) | Median (midwater) | 211 | 120 | 180 | 212 | 142 | 193 |
| | Median (seabed) | 203 | 109 | 169 | 209 | 138 | 191 |
| | Change (midwater) | | -92 | -32 | | -70 | -19 |
| | Change (seabed) | | -94 | -35 | | -71 | -19 |
| Euphotic zone depth | Median (m) | 23.1 | 15.4 | 19.5 | 23.2 | 17.2 | 20.8 |
| | Change (%) | | -33.1 | -15.4 | | -25.6 | -10.5 |
| >1% light at seabed | Median (days per year) | 200 | 84 | 147 | 201 | 115 | 168 |
| | Change (days per year) | | -116 | -53 | | -86 | -32 |

2.7.2 Graham Bank: Predicted optical effects

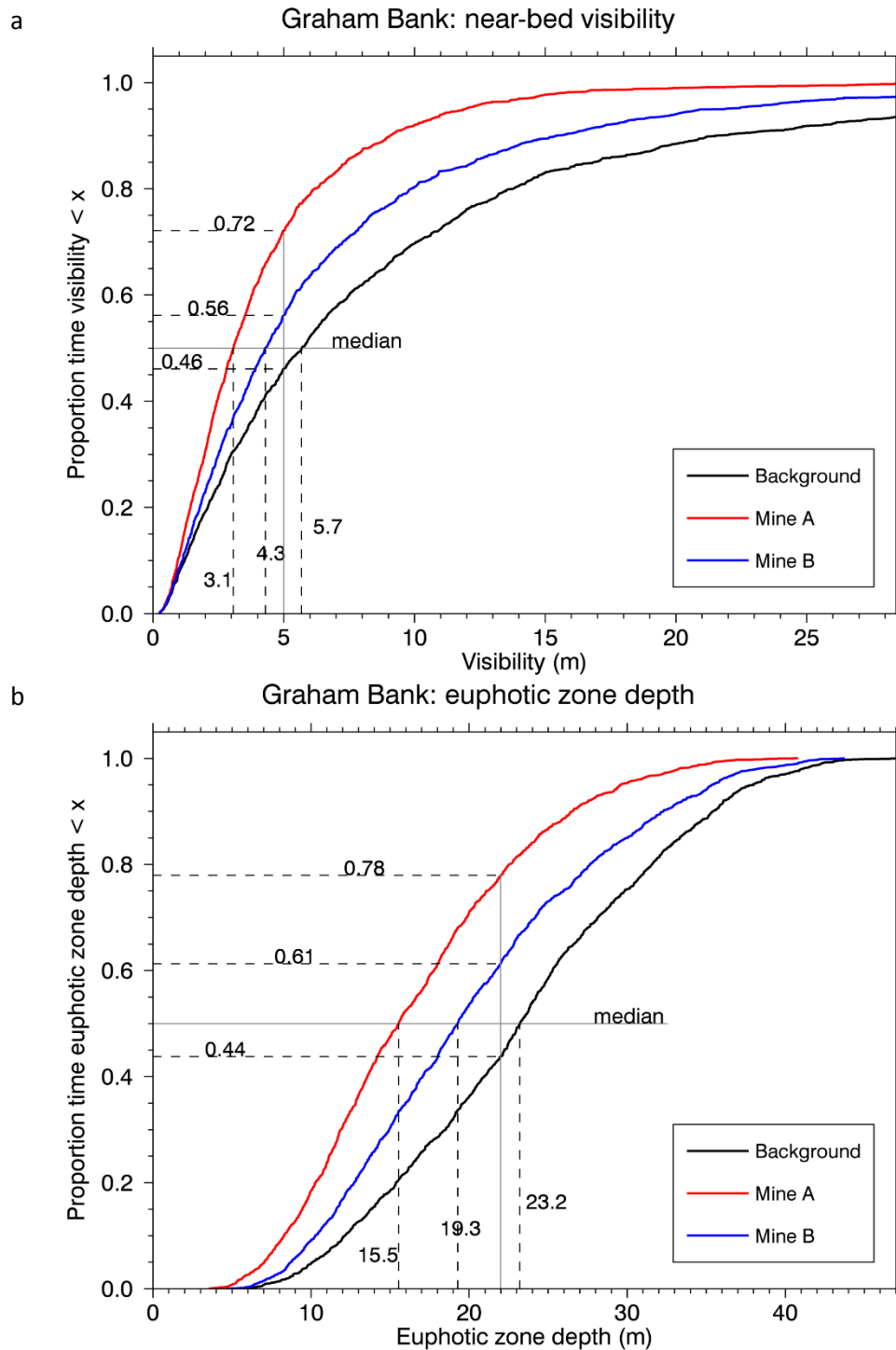


Figure 2-15. Graham Bank: Predicted effects of mining on cumulative distribution of near bed visibility and euphotic zone depth. Background (no mining) – black; Mining at site A – red; Mining at site B – blue. Dashed lines show the median values and the proportions of time for which the euphotic zone depth is less than the depth of the seabed.

Table 2-5: Graham Bank: Predicted optical properties. Predicted optical properties and their changes from background conditions if iron-sand recovery operations took place at the inner (Site A) or outer (Site B) end of the proposed mining area. For comparison, results based on the optical modelling of Pinkerton & Gall (2015) are shown and shaded grey.

| | | Present study | | | Pinkerton & Gall (2015) | | |
|--------------------------------------|------------------------|---------------|--------|--------|-------------------------|--------|--------|
| Metric | | Back-ground | Site A | Site B | Back-ground | Site A | Site B |
| Horizontal visibility | Median (midwater) (m) | 6.1 | 3.3 | 4.6 | 6.1 | 3.9 | 5.1 |
| | Median (seabed) (m) | 5.7 | 3.1 | 4.3 | 5.9 | 3.7 | 5.0 |
| | Change (midwater) (%) | | -45.2 | -23.3 | | -36.5 | -17.0 |
| | Change (seabed) (%) | | -46.1 | -24.5 | | -37.1 | -15.7 |
| High visibility days (days per year) | Median (midwater) | 208 | 114 | 171 | 207 | 140 | 185 |
| | Median (seabed) | 197 | 102 | 160 | 204 | 133 | 180 |
| | Change (midwater) | | -94 | -37 | | -67 | -22 |
| | Change (seabed) | | -95 | -37 | | -71 | -24 |
| Euphotic zone depth | Median (m) | 23.2 | 15.5 | 19.3 | 23.3 | 17.6 | 20.5 |
| | Change (%) | | -33.0 | -17.0 | | -24.1 | -11.9 |
| >1% light at seabed | Median (days per year) | 205 | 81 | 141 | 206 | 111 | 159 |
| | Change (days per year) | | -125 | -64 | | -95 | -47 |

2.7.3 The Crack 1: Predicted optical effects

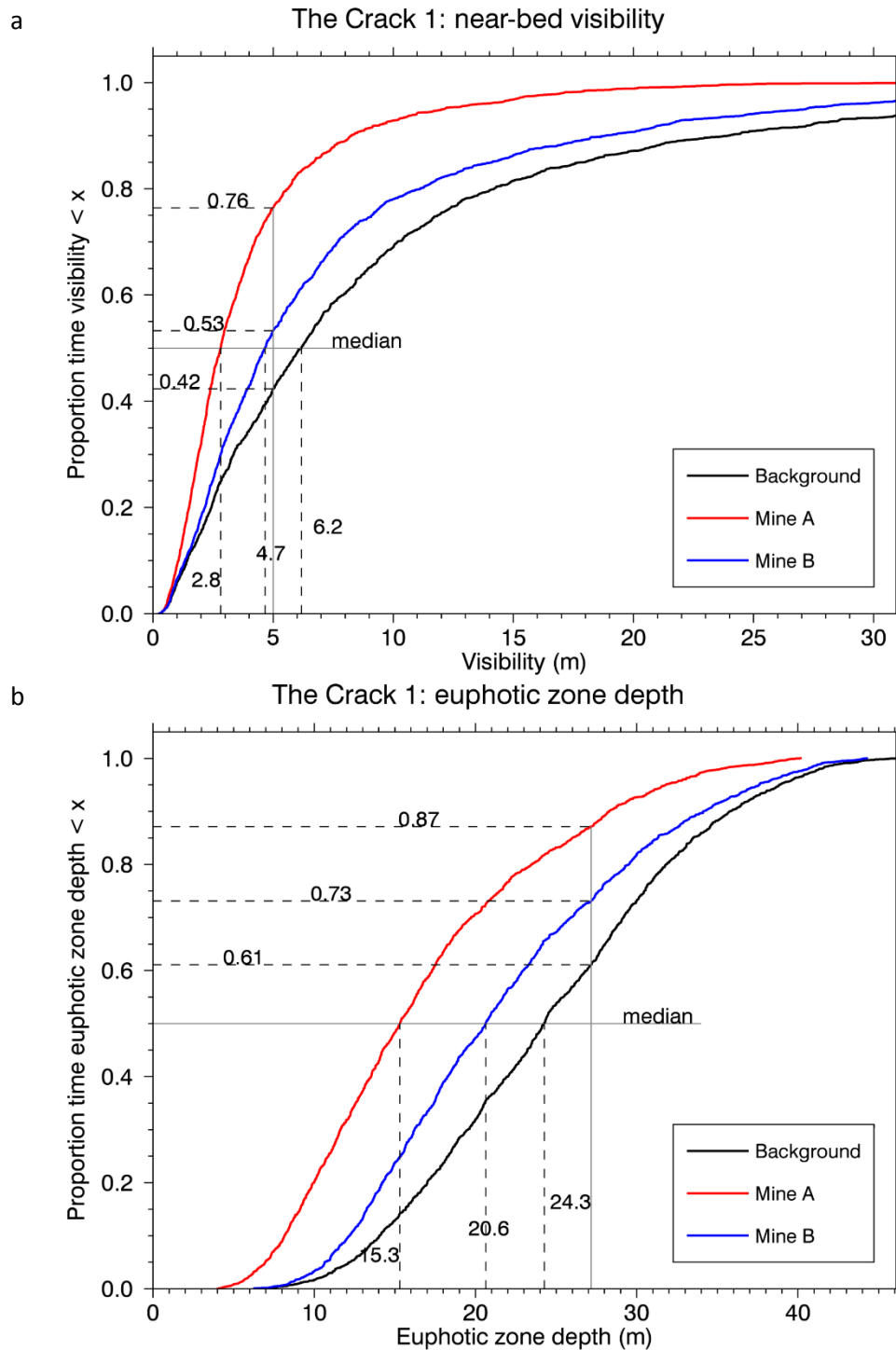


Figure 2-16. The Crack 1: Predicted effects of mining on cumulative distribution of near bed visibility and euphotic zone depth. Background (no mining) – black; Mining at site A – red; Mining at site B – blue. Dashed lines show the median values and the proportions of time for which the euphotic zone depth is less than the depth of the seabed.

Table 2-6: The Crack 1: Predicted optical properties. Predicted optical properties and their changes from background conditions if iron-sand recovery operations took place at the inner (Site A) or outer (Site B) end of the proposed mining area. For comparison, results based on the optical modelling of Pinkerton & Gall (2015) are shown and shaded grey.

| The Crack 1 | Metric | Present study | | | Pinkerton & Gall (2015) | | |
|--------------------------------------|------------------------|---------------|--------|--------|-------------------------|--------|--------|
| | | Back-ground | Site A | Site B | Back-ground | Site A | Site B |
| Horizontal visibility | Median (midwater) (m) | 6.9 | 3.2 | 5.3 | 7.0 | 3.7 | 5.8 |
| | Median (seabed) (m) | 6.2 | 2.8 | 4.7 | 6.4 | 3.4 | 5.3 |
| | Change (midwater) (%) | | -54.5 | -23.6 | | -46.5 | -17.2 |
| | Change (seabed) (%) | | -54.4 | -24.6 | | -47.1 | -17.1 |
| High visibility days (days per year) | Median (midwater) | 229 | 108 | 192 | 229 | 132 | 205 |
| | Median (seabed) | 211 | 86 | 171 | 216 | 114 | 191 |
| | Change (midwater) | | -121 | -37 | | -98 | -25 |
| | Change (seabed) | | -124 | -40 | | -102 | -25 |
| Euphotic zone depth | Median (m) | 24.3 | 15.3 | 20.6 | 24.3 | 17.0 | 21.8 |
| | Change (%) | | -36.9 | -14.9 | | -29.9 | -10.4 |
| >1% light at seabed | Median (days per year) | 142 | 47 | 98 | 143 | 56 | 109 |
| | Change (days per year) | | -95 | -44 | | -87 | -34 |

2.7.4 The Crack 2: Predicted optical effects at Patea

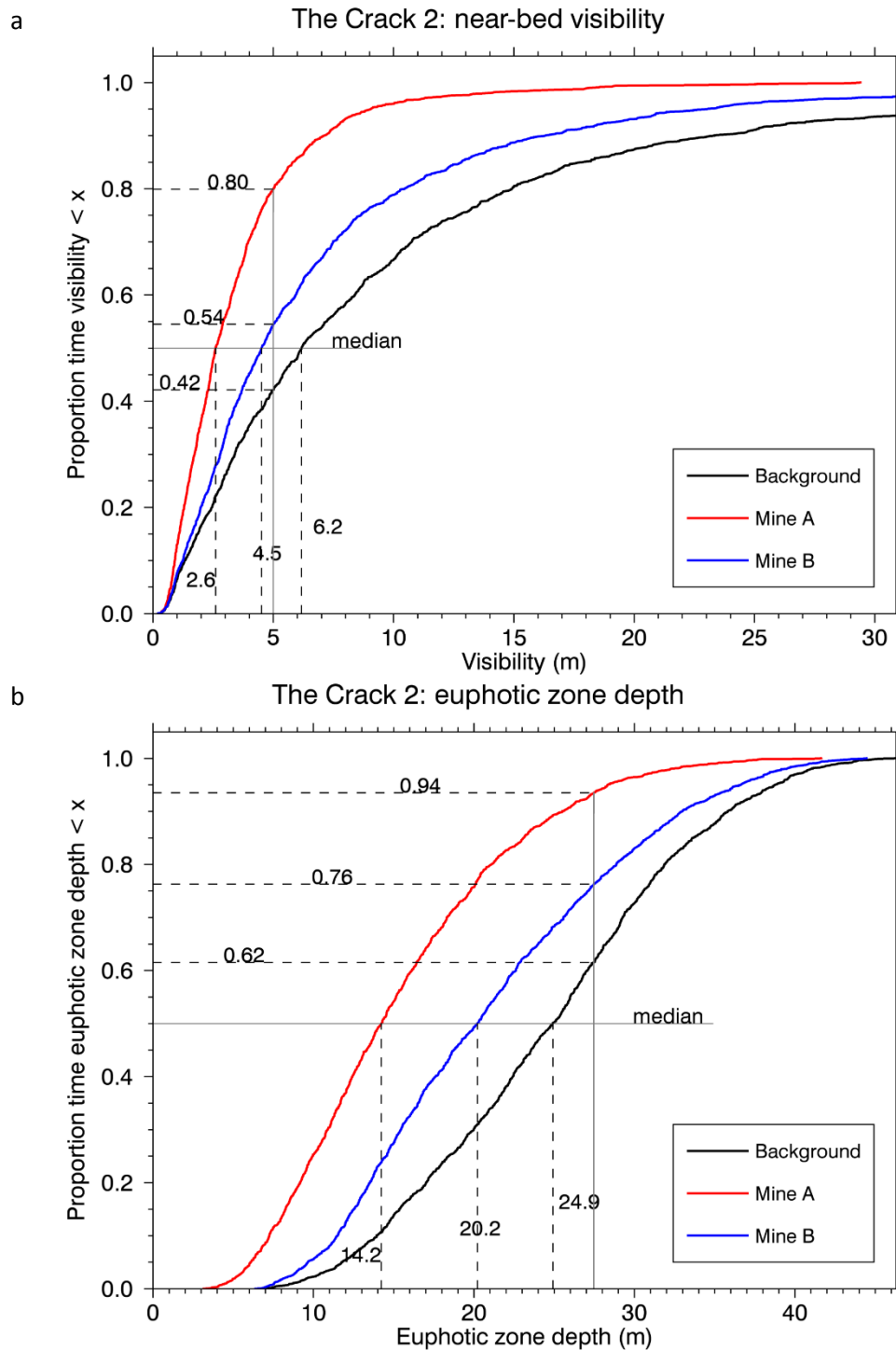


Figure 2-17. The Crack 2: Predicted effects of mining on cumulative distribution of near bed visibility and euphotic zone depth. Background (no mining) – black; Mining at site A – red; Mining at site B – blue. Dashed lines show the median values and the proportions of time for which the euphotic zone depth is less than the depth of the seabed.

Table 2-7: The Crack 2: Predicted optical properties. Predicted optical properties and their changes from background conditions if iron-sand recovery operations took place at the inner (Site A) or outer (Site B) end of the proposed mining area. For comparison, results based on the optical modelling of Pinkerton & Gall (2015) are shown and shaded grey.

| The Crack 2 | Metric | Present study | | | Pinkerton & Gall (2015) | | |
|--------------------------------------|------------------------|---------------|--------|--------|-------------------------|--------|--------|
| | | Back-ground | Site A | Site B | Back-ground | Site A | Site B |
| Horizontal visibility | Median (midwater) (m) | 6.7 | 2.9 | 4.9 | 6.7 | 3.5 | 5.3 |
| | Median (seabed) (m) | 6.2 | 2.6 | 4.5 | 6.4 | 3.3 | 5.1 |
| | Change (midwater) (%) | | -57.3 | -27.1 | | -47.3 | -20.7 |
| | Change (seabed) (%) | | -57.9 | -27.0 | | -48.3 | -20.2 |
| High visibility days (days per year) | Median (midwater) | 220 | 87 | 179 | 221 | 114 | 194 |
| | Median (seabed) | 211 | 73 | 166 | 215 | 103 | 185 |
| | Change (midwater) | | -133 | -41 | | -107 | -27 |
| | Change (seabed) | | -138 | -45 | | -112 | -30 |
| Euphotic zone depth | Median (m) | 24.9 | 14.2 | 20.2 | 25.0 | 16.5 | 21.6 |
| | Change (%) | | -42.9 | -18.9 | | -34.2 | -13.5 |
| >1% light at seabed | Median (days per year) | 140 | 24 | 87 | 141 | 38 | 97 |
| | Change (days per year) | | -117 | -54 | | -102 | -43 |

2.7.5 North Traps: Predicted optical effects

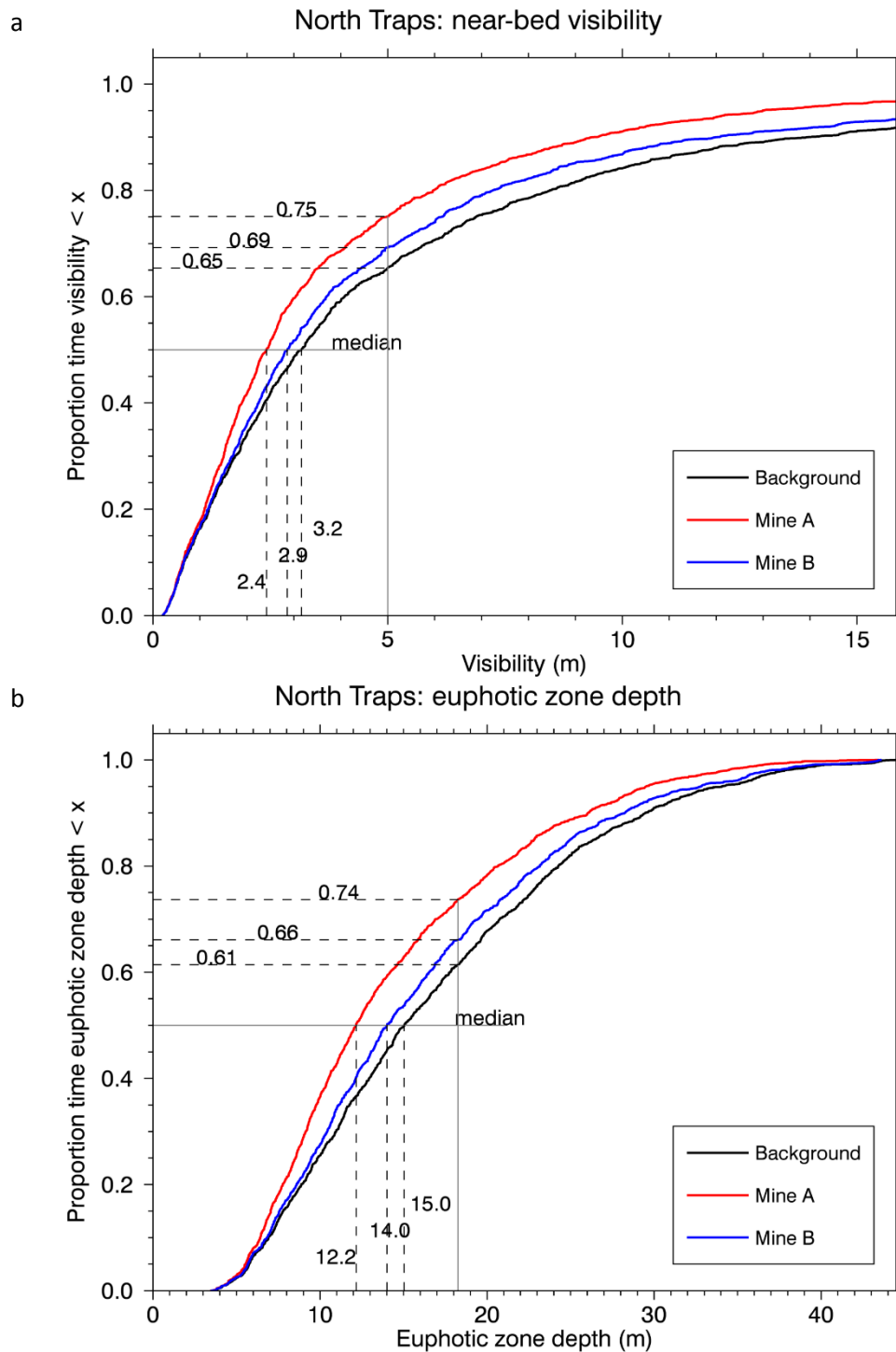


Figure 2-18. North Traps: Predicted effects of mining on cumulative distribution of near bed visibility and euphotic zone depth. Background (no mining) – black; Mining at site A – red; Mining at site B – blue. Dashed lines show the median values and the proportions of time for which the euphotic zone depth is less than the depth of the seabed.

Table 2-8: North Traps: Predicted optical properties. Predicted optical properties and their changes from background conditions if iron-sand recovery operations took place at the inner (Site A) or outer (Site B) end of the proposed mining area. For comparison, results based on the optical modelling of Pinkerton & Gall (2015) are shown and shaded grey.

| North Traps | Metric | Present study | | | Pinkerton & Gall (2015) | | |
|--------------------------------------|------------------------|---------------|--------|--------|-------------------------|--------|--------|
| | | Back-ground | Site A | Site B | Back-ground | Site A | Site B |
| Horizontal visibility | Median (midwater) (m) | 3.4 | 2.6 | 3.1 | 3.5 | 2.9 | 3.2 |
| | Median (seabed) (m) | 3.2 | 2.4 | 2.9 | 3.5 | 2.9 | 3.3 |
| | Change (midwater) (%) | | -24.8 | -7.9 | | -17.1 | -6.2 |
| | Change (seabed) (%) | | -23.7 | -9.7 | | -17.1 | -6.6 |
| High visibility days (days per year) | Median (midwater) | 134 | 100 | 122 | 134 | 108 | 128 |
| | Median (seabed) | 126 | 91 | 112 | 136 | 106 | 130 |
| | Change (midwater) | | -34 | -12 | | -26 | -7 |
| | Change (seabed) | | -35 | -14 | | -30 | -7 |
| Euphotic zone depth | Median (m) | 15.0 | 12.2 | 14.0 | 15.1 | 13.3 | 14.5 |
| | Change (%) | | -19.2 | -6.9 | | -12.1 | -4.4 |
| >1% light at seabed | Median (days per year) | 141 | 96 | 124 | 142 | 108 | 130 |
| | Change (days per year) | | -45 | -17 | | -34 | -11 |

2.7.6 Rolling Grounds: Predicted optical effects

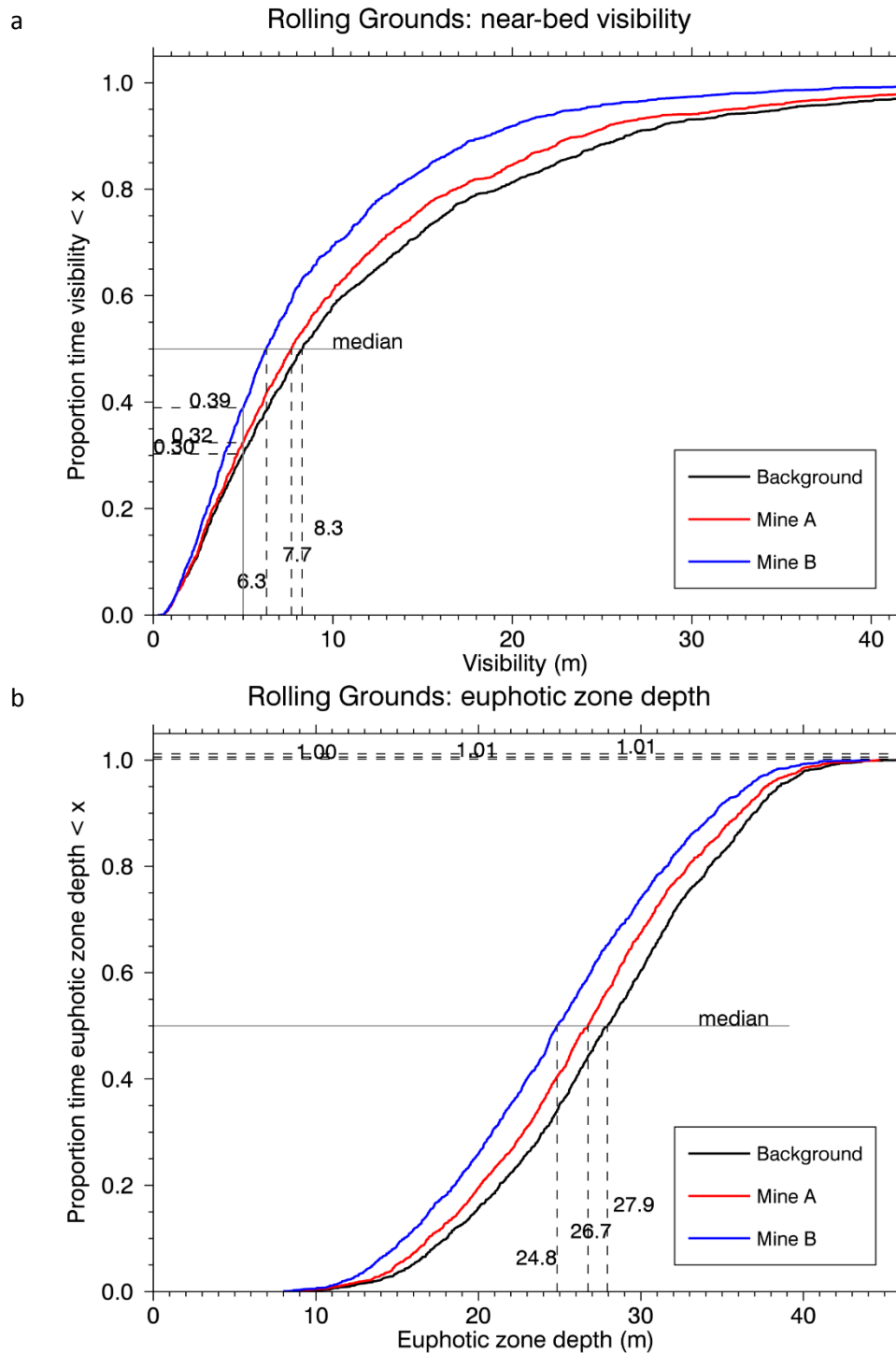


Figure 2-19. Rolling Grounds: Predicted effects of mining on cumulative distribution of near bed visibility and euphotic zone depth. Background (no mining) – black; Mining at site A – red; Mining at site B – blue. Dashed lines show the median values and the proportions of time for which the euphotic zone depth is less than the depth of the seabed.

Table 2-9: Rolling Grounds: Predicted optical properties. Predicted optical properties and their changes from background conditions if iron-sand recovery operations took place at the inner (Site A) or outer (Site B) end of the proposed mining area. For comparison, results based on the optical modelling of Pinkerton & Gall (2015) are shown and shaded grey.

| Rolling Grounds | Metric | Present study | | | Pinkerton & Gall (2015) | | |
|--------------------------------------|------------------------|---------------|--------|--------|-------------------------|--------|--------|
| | | Back-ground | Site A | Site B | Back-ground | Site A | Site B |
| Horizontal visibility | Median (midwater) (m) | 9.1 | 8.4 | 7.0 | 9.1 | 8.7 | 7.7 |
| | Median (seabed) (m) | 8.3 | 7.7 | 6.3 | 8.5 | 8.1 | 7.1 |
| | Change (midwater) (%) | | -7.3 | -22.7 | | -4.7 | -15.6 |
| | Change (seabed) (%) | | -7.3 | -24.0 | | -4.5 | -17.2 |
| High visibility days (days per year) | Median (midwater) | 262 | 254 | 239 | 262 | 258 | 249 |
| | Median (seabed) | 255 | 247 | 223 | 257 | 253 | 239 |
| | Change (midwater) | | -8 | -23 | | -5 | -14 |
| | Change (seabed) | | -8 | -32 | | -4 | -18 |
| Euphotic zone depth | Median (m) | 27.9 | 26.7 | 24.8 | 28.0 | 27.2 | 25.8 |
| | Change (%) | | -4.3 | -11.1 | | -2.8 | -7.8 |
| >1% light at seabed | Median (days per year) | -1 | -4 | -2 | -1 | -1 | -1 |
| | Change (days per year) | | -4 | -1 | | 0 | 0 |

2.7.7 Project Reef: Predicted optical effects

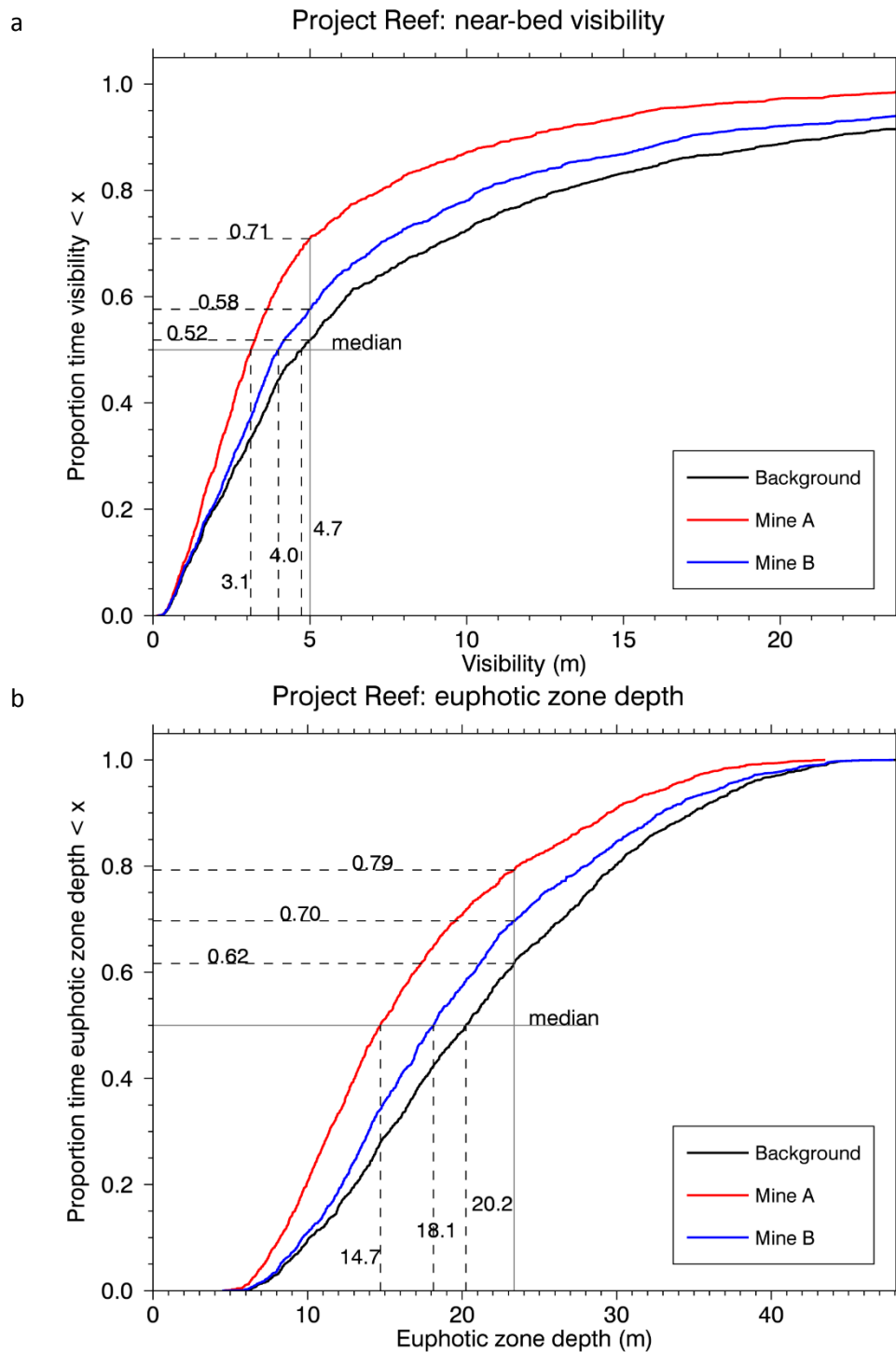


Figure 2-20. Project Reef: Predicted effects of mining on cumulative distribution of near bed visibility and euphotic zone depth. Background (no mining) – black; Mining at site A – red; Mining at site B – blue. Dashed lines show the median values and the proportions of time for which the euphotic zone depth is less than the depth of the seabed.

Table 2-10: Project Reef: Predicted optical properties. Predicted optical properties and their changes from background conditions if iron-sand recovery operations took place at the inner (Site A) or outer (Site B) end of the proposed mining area. For comparison, results based on the optical modelling of Pinkerton & Gall (2015) are shown and shaded grey.

| Project Reef | Metric | Present study | | | Pinkerton & Gall (2015) | | |
|--------------------------------------|------------------------|---------------|--------|--------|-------------------------|--------|--------|
| | | Back-ground | Site A | Site B | Back-ground | Site A | Site B |
| Horizontal visibility | Median (midwater) (m) | 5.2 | 3.4 | 4.4 | 5.2 | 3.9 | 4.7 |
| | Median (seabed) (m) | 4.7 | 3.1 | 4.0 | 5.1 | 3.7 | 4.5 |
| | Change (midwater) (%) | | -34.1 | -14.9 | | -24.9 | -10.5 |
| | Change (seabed) (%) | | -34.2 | -15.7 | | -28.1 | -11.6 |
| High visibility days (days per year) | Median (midwater) | 189 | 119 | 166 | 189 | 137 | 175 |
| | Median (seabed) | 176 | 106 | 155 | 186 | 129 | 167 |
| | Change (midwater) | | -70 | -22 | | -52 | -14 |
| | Change (seabed) | | -70 | -21 | | -57 | -19 |
| Euphotic zone depth | Median (m) | 20.2 | 14.7 | 18.1 | 20.3 | 16.2 | 19.0 |
| | Change (%) | | -27.3 | -10.3 | | -20.4 | -6.7 |
| >1% light at seabed | Median (days per year) | 140 | 76 | 111 | 142 | 92 | 123 |
| | Change (days per year) | | -64 | -29 | | -50 | -19 |

2.7.8 Source A North 20: Predicted optical effects

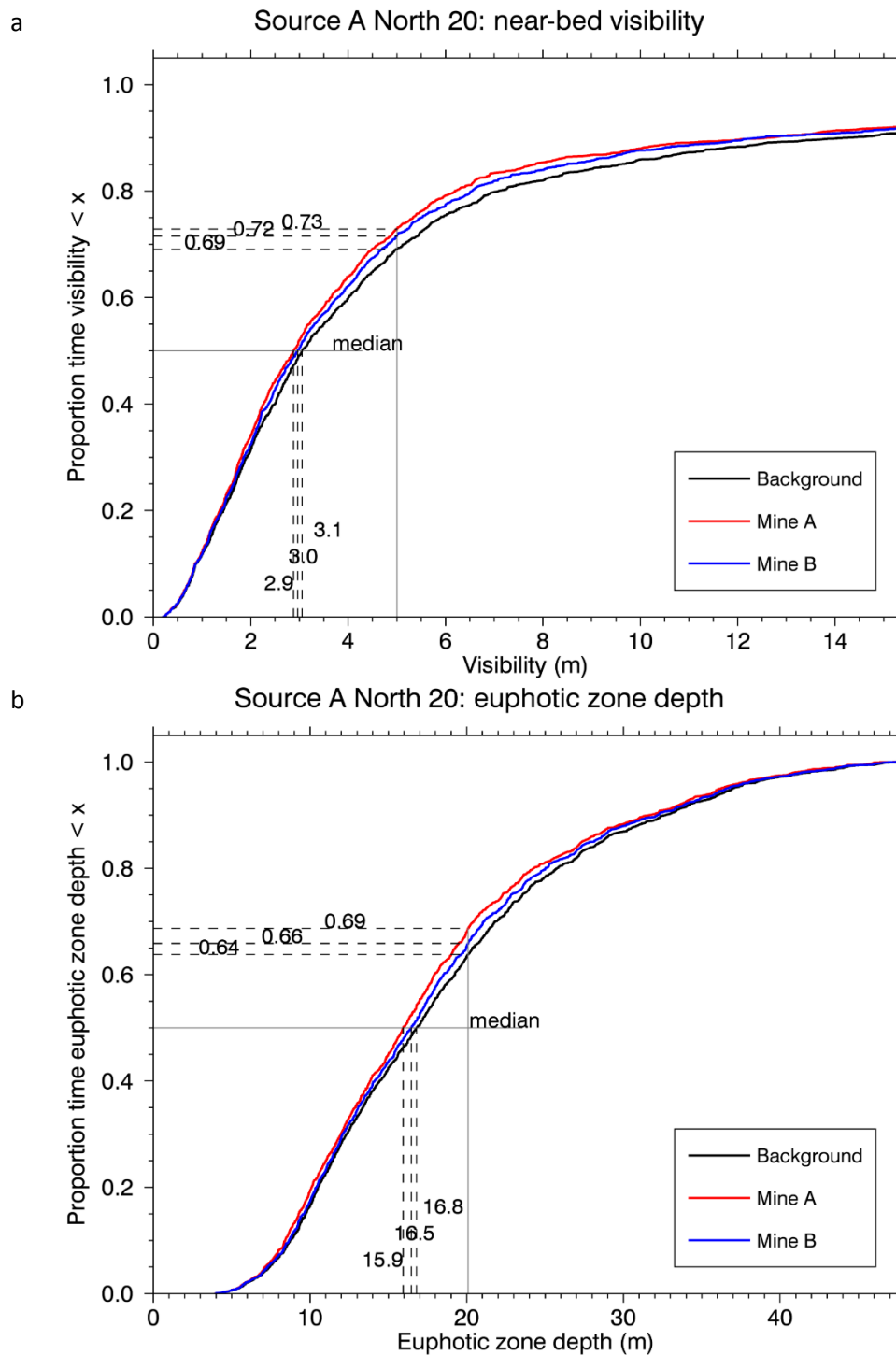


Figure 2-21. Source A North 20: Predicted effects of mining on cumulative distribution of near bed visibility and euphotic zone depth. Background (no mining) – black; Mining at site A – red; Mining at site B – blue. Dashed lines show the median values and the proportions of time for which the euphotic zone depth is less than the depth of the seabed.

Table 2-11: Source A North 20: Predicted optical properties. Predicted optical properties and their changes from background conditions if iron-sand recovery operations took place at the inner (Site A) or outer (Site B) end of the proposed mining area. For comparison, results based on the optical modelling of Pinkerton & Gall (2015) are shown and shaded grey.

| Source A North 20 | | Present study | | | Pinkerton & Gall (2015) | | |
|--------------------------------------|------------------------|---------------|--------|--------|-------------------------|--------|--------|
| | | Back-ground | Site A | Site B | Back-ground | Site A | Site B |
| Horizontal visibility | Median (midwater) (m) | 3.8 | 3.5 | 3.6 | 3.8 | 3.6 | 3.7 |
| | Median (seabed) (m) | 3.1 | 2.9 | 3.0 | 3.3 | 3.1 | 3.2 |
| | Change (midwater) (%) | | -6.7 | -4.3 | | -4.8 | -2.2 |
| | Change (seabed) (%) | | -5.9 | -3.2 | | -6.3 | -4.7 |
| High visibility days (days per year) | Median (midwater) | 146 | 133 | 138 | 147 | 137 | 141 |
| | Median (seabed) | 113 | 99 | 104 | 121 | 111 | 112 |
| | Change (midwater) | | -13 | -7 | | -9 | -5 |
| | Change (seabed) | | -14 | -9 | | -10 | -9 |
| Euphotic zone depth | Median (m) | 16.8 | 15.9 | 16.5 | 16.9 | 16.5 | 16.7 |
| | Change (%) | | -5.1 | -1.9 | | -2.8 | -1.3 |
| >1% light at seabed | Median (days per year) | 132 | 114 | 125 | 135 | 124 | 131 |
| | Change (days per year) | | -18 | -8 | | -10 | -4 |

3 Discussion and conclusions

3.1.1 Predicted optical effects

This re-analysis and report summarises the optical effects of proposed mining in the South Taranaki Bight (STB) under “worst-case” scenario. The predicted optical effects in the new “worst case” simulations are qualitatively similar to those from Pinkerton & Gall (2015), but quantitatively greater (Table 3-1). Averaged across the sediment model domain, optical effects that are relevant to estimating effects on primary productivity were 43.8% greater in the new simulations than estimated using the models summarised in Pinkerton & Gall (2015). This considered effects of mining on mean light in the water column, mean light at the seabed, and the number of days per year when seabed light was greater than two ecologically-relevant limits (0.04 and 0.4 mol/m²/d).

At the scale of the sediment model domain, predicted optical effects of mining are 23% greater due to mining at site A than site B in the new worst-case simulations (compared to 26% greater due to mining at site A than site B in Pinkerton & Gall 2015).

The significance of these simulated optical effects of mining for primary production by phytoplankton and microphytobenthos in the STB (cf. Cahoon et al., 2015) are not considered explicitly in the present report.

Table 3-1: Simulated optical effects of mining of relevance to effects on primary productivity. Comparison of effects in the present "worst-case" simulations [x] and in Pinkerton & Gall (2015) [y], where the last column: "Difference" = $100 \cdot (x-y)/y$. E=incident broadband irradiance (mol/m²/d).

| Measure | Mean change over sediment model domain | Present study | | Pinkerton & Gall (2015) | | Difference (%) | |
|---|--|---------------|--------|-------------------------|--------|----------------|--------|
| | | mine A | mine B | mine A | mine B | mine A | mine B |
| Water column light | Mean change total (%) | -2.9 | -2.4 | -1.9 | -1.6 | 49.3 | 51.5 |
| Light at the seabed | Change in area with E>0.04 (%) | -10.3 | -9.3 | -6.8 | -6.0 | 50.3 | 57.0 |
| | Change in area with E>0.4 (%) | -22.7 | -19.1 | -16.5 | -13.8 | 37.3 | 38.0 |
| | Mean change total (%) | -30.0 | -21.0 | -22.8 | -15.5 | 31.8 | 35.4 |
| Mean change due to mine A/mean change due to mine B | | | 1.23 | | 1.26 | | |
| Average (by site of mining) | | | | | | 42.2 | 45.5 |
| Average (across both sites) | | | | | | | 43.8 |

3.1.2 Optical effects at selected stations

On average, optical effects of mining at the selected 8 sites are 41.0% greater in the new simulations than estimated using the models summarised in Pinkerton & Gall (2015). This considers four optical effects: horizontal visibility (midwater and seabed), number of high visibility days per year (in midwater and at seabed), euphotic zone depth, and number of days per year with >1% light at the seabed (Table 3-2).

The changes in the predicted optical effects between the present "worst-case" study and Pinkerton & Gall (2015) varies between stations. Changes at The Crack 2 are 29.6% greater under the worst-case simulations than Pinkerton & Gall (2015), whereas changes to the predicted optical effects at the Rolling Grounds are 57.9% greater under the worst-case simulations than Pinkerton & Gall (2015).

The predicted optical effects of mining at all stations except one (Rolling Grounds) are 2.19 times greater for mining at site A than for mining at site B in the new "worst-case" simulations (compared to 2.45 times consistent with Pinkerton & Gall, 2015). This arises because the predicted effects under the "worst-case" simulation are 33.5% greater (averaged over all stations) than Pinkerton & Gall (2015) for mining at site A, and 48.6% greater (averaged over all stations) than Pinkerton & Gall (2015) for mining at site B.

Table 3-2: Simulated optical effects of mining at selected stations. Comparison of effects in the present "worst-case" simulations [x] and in Pinkerton & Gall (2015) [y], where the column marked: "Difference" = $100*(x-y)/y$. "Station average" is the average change between this study and Pinkerton & Gall (2015) at a given station for mining at both site A and site B, considering all six optical properties.

| Station | Change in optical property | Present study | | Pinkerton & Gall (2015) | | Difference (%) | | Station average |
|---------------------------|---------------------------------------|---------------|--------|-------------------------|--------|----------------|--------|-----------------|
| | | Site A | Site B | Site A | Site B | Site A | Site B | |
| Source A to Whang-anui 20 | Horizontal visibility (midwater) (%) | -47.1 | -24.6 | -38.9 | -16.5 | 21.1 | 49.5 | 43.0 |
| | Horizontal visibility (seabed) | -45.3 | -22.6 | -39.9 | -15.4 | 13.5 | 46.2 | |
| | High visibility days (midwater) (d/y) | -91.6 | -31.8 | -70.4 | -19.3 | 30.2 | 64.5 | |
| | High visibility days (seabed) (d/y) | -94.2 | -34.8 | -71.5 | -18.9 | 31.8 | 84.4 | |
| | Euphotic zone depth (%) | -33.1 | -15.4 | -25.6 | -10.5 | 29.1 | 47.6 | |
| | Days with >1% light at seabed (d/y) | -115.9 | -52.9 | -85.8 | -32.4 | 35.1 | 63.7 | |
| Graham Bank | Horizontal visibility (midwater) (%) | -45.2 | -23.3 | -36.5 | -17.0 | 23.9 | 37.1 | 40.4 |
| | Horizontal visibility (seabed) | -46.1 | -24.5 | -37.1 | -15.7 | 24.3 | 55.7 | |
| | High visibility days (midwater) (d/y) | -93.7 | -37.0 | -66.9 | -21.9 | 40.2 | 68.5 | |
| | High visibility days (seabed) (d/y) | -95.0 | -36.8 | -70.8 | -24.0 | 34.2 | 53.5 | |
| | Euphotic zone depth (%) | -33.0 | -17.0 | -24.1 | -11.9 | 36.9 | 43.4 | |
| | Days with >1% light at seabed (d/y) | -124.8 | -64.0 | -95.4 | -46.8 | 30.8 | 36.6 | |
| The Crack 1 | Horizontal visibility (midwater) (%) | -54.5 | -23.6 | -46.5 | -17.2 | 17.3 | 37.3 | 31.6 |
| | Horizontal visibility (seabed) | -54.4 | -24.6 | -47.1 | -17.1 | 15.4 | 43.8 | |
| | High visibility days (midwater) (d/y) | -121.0 | -37.0 | -97.6 | -24.6 | 23.9 | 50.3 | |
| | High visibility days (seabed) (d/y) | -124.5 | -40.0 | -101.8 | -24.6 | 22.3 | 62.8 | |
| | Euphotic zone depth (%) | -36.9 | -14.9 | -29.9 | -10.4 | 23.5 | 42.9 | |
| | Days with >1% light at seabed (d/y) | -95.1 | -43.9 | -86.9 | -33.7 | 9.5 | 30.4 | |
| The Crack 2 | Horizontal visibility (midwater) (%) | -57.3 | -27.1 | -47.3 | -20.7 | 21.1 | 31.0 | 29.6 |
| | Horizontal visibility (seabed) | -57.9 | -27.0 | -48.3 | -20.2 | 19.8 | 33.4 | |
| | High visibility days (midwater) (d/y) | -132.7 | -40.7 | -107.4 | -27.1 | 23.6 | 50.5 | |
| | High visibility days (seabed) (d/y) | -137.9 | -45.0 | -112.2 | -30.2 | 22.9 | 49.2 | |
| | Euphotic zone depth (%) | -42.9 | -18.9 | -34.2 | -13.5 | 25.5 | 40.3 | |
| | Days with >1% light at seabed (d/y) | -116.8 | -53.8 | -102.4 | -43.4 | 14.0 | 24.2 | |

Table 3-2. Continued

| Station | Change in optical property | Present study | | Pinkerton & Gall (2015) | | Difference (%) | | Station average |
|---|---------------------------------------|---------------|--------|-------------------------|--------|----------------|--------|-----------------|
| | | Site A | Site B | Site A | Site B | Site A | Site B | |
| North Traps | Horizontal visibility (midwater) (%) | -24.8 | -7.9 | -17.1 | -6.2 | 45.4 | 27.7 | 49.9 |
| | Horizontal visibility (seabed) | -23.7 | -9.7 | -17.1 | -6.6 | 38.5 | 46.3 | |
| | High visibility days (midwater) (d/y) | -34.2 | -11.9 | -25.8 | -6.7 | 32.8 | 78.6 | |
| | High visibility days (seabed) (d/y) | -35.4 | -14.1 | -29.9 | -6.6 | 18.5 | 113.6 | |
| | Euphotic zone depth (%) | -19.2 | -6.9 | -12.1 | -4.4 | 58.8 | 56.4 | |
| | Days with >1% light at seabed (d/y) | -44.8 | -17.2 | -33.9 | -11.5 | 32.4 | 50.0 | |
| Rolling Grounds | Horizontal visibility (midwater) (%) | -7.3 | -22.7 | -4.7 | -15.6 | 56.6 | 45.8 | 57.9 |
| | Horizontal visibility (seabed) | -7.3 | -24.0 | -4.5 | -17.2 | 63.2 | 39.7 | |
| | High visibility days (midwater) (d/y) | -7.8 | -22.9 | -4.8 | -13.9 | 62.2 | 64.8 | |
| | High visibility days (seabed) (d/y) | -7.9 | -31.7 | -4.4 | -18.3 | 77.1 | 73.9 | |
| | Euphotic zone depth (%) | -4.3 | -11.1 | -2.8 | -7.8 | 53.3 | 42.9 | |
| | Days with >1% light at seabed (d/y) | -3.6 | -1.3 | -0.1 | -0.3 | NA | NA | |
| Project Reef | Horizontal visibility (midwater) (%) | -34.1 | -14.9 | -24.9 | -10.5 | 36.5 | 42.4 | 37.1 |
| | Horizontal visibility (seabed) | -34.2 | -15.7 | -28.1 | -11.6 | 21.9 | 35.3 | |
| | High visibility days (midwater) (d/y) | -70.2 | -22.5 | -51.8 | -13.9 | 35.5 | 61.9 | |
| | High visibility days (seabed) (d/y) | -69.8 | -21.3 | -56.5 | -18.6 | 23.5 | 15.0 | |
| | Euphotic zone depth (%) | -27.3 | -10.3 | -20.4 | -6.7 | 33.9 | 54.9 | |
| | Days with >1% light at seabed (d/y) | -64.3 | -29.3 | -49.7 | -18.9 | 29.4 | 55.2 | |
| Source A North 20 | Horizontal visibility (midwater) (%) | -6.7 | -4.3 | -4.8 | -2.2 | 38.6 | 94.4 | 41.4 |
| | Horizontal visibility (seabed) | -5.9 | -3.2 | -6.3 | -4.7 | -6.8 | -31.2 | |
| | High visibility days (midwater) (d/y) | -12.7 | -7.4 | -9.2 | -5.3 | 38.6 | 38.7 | |
| | High visibility days (seabed) (d/y) | -13.9 | -9.1 | -9.9 | -9.4 | 41.0 | -3.5 | |
| | Euphotic zone depth (%) | -5.1 | -1.9 | -2.8 | -1.3 | 82.5 | 48.0 | |
| | Days with >1% light at seabed (d/y) | -17.9 | -7.5 | -10.5 | -4.1 | 71.1 | 85.0 | |
| Mean change due to mine A/mean change due to mine B | | | 2.19 | | 2.45 | | | |
| Average (by site of mining) | | | | | | 33.5 | 48.6 | |
| Average (across both sites) | | | | | | | 41.0 | |

4 Acknowledgements

Helen Macdonald and Mark Hadfield (NIWA) provided sediment model data, and also generated the “movie” files of pseudo-true colour. Mark Gall produced Figures 2-4 and 2-5. I thank Alison MacDiarmid (NIWA) for review and comments.

5 References

Cahoon, L. (2014). Photo-adaptation by Microphytobenthos. Comment to TTR, received by email 29 October 2014. Pp 5.

- Cahoon, L.B.; M.H. Pinkerton; I. Hawes (2015). Effects on primary production of proposed iron-sand mining in the South Taranaki Bight region. Report for Trans-Tasman Resources, Ltd. Pp 30.
- Falkowski, P.G.; J.A. Raven (1997). Aquatic Photosynthesis. Blackwell Science, Inc., Massachusetts. Pp 360.
- Huettel, M.P. Berg; J.E. Kostka. (2014). Benthic Exchange and Biogeochemical Cycling in Permeable Sediments. Annual Reviews of Marine Science, 6: 23-51.
- Kirk, J.T.O. (2011) Light and photosynthesis in aquatic ecosystems. Cambridge University Press, Cambridge. Pp 649. Cahoon, L.B.; M.H. Pinkerton; I. Hawes (2015). Effects on primary production of proposed iron-sand mining in the South Taranaki Bight region. Report for Trans-Tasman Resources, Ltd. Pp 30.
- Macdonald, H.; M. Hadfield (2017). South Taranaki Bight Sediment Plume Modelling: Worst Case Scenario. NIWA client report 2017049WN for Trans-Tasman Resources. March 2017.
- Pinkerton, M.H.; M. Gall (2015). Optical effects of proposed iron-sand mining in the South Taranaki Bight region. NIWA client report WLG2015-26 rev 2 for Trans-Tasman Resources. Project TTR15301.